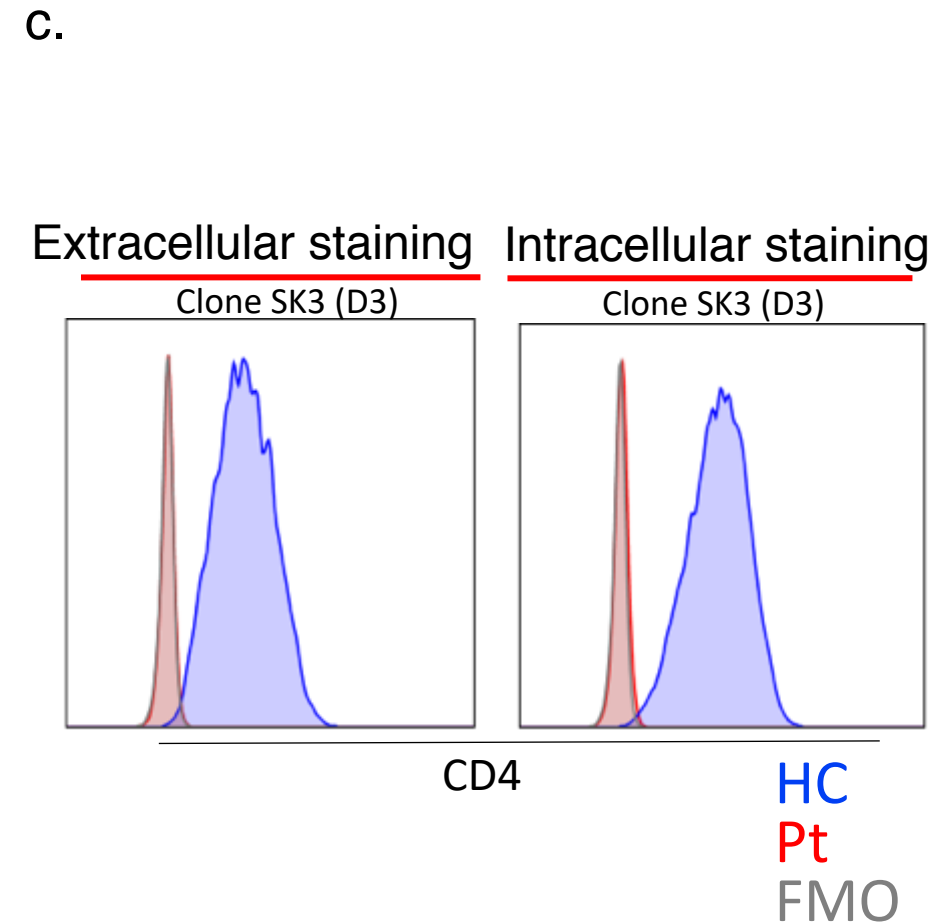
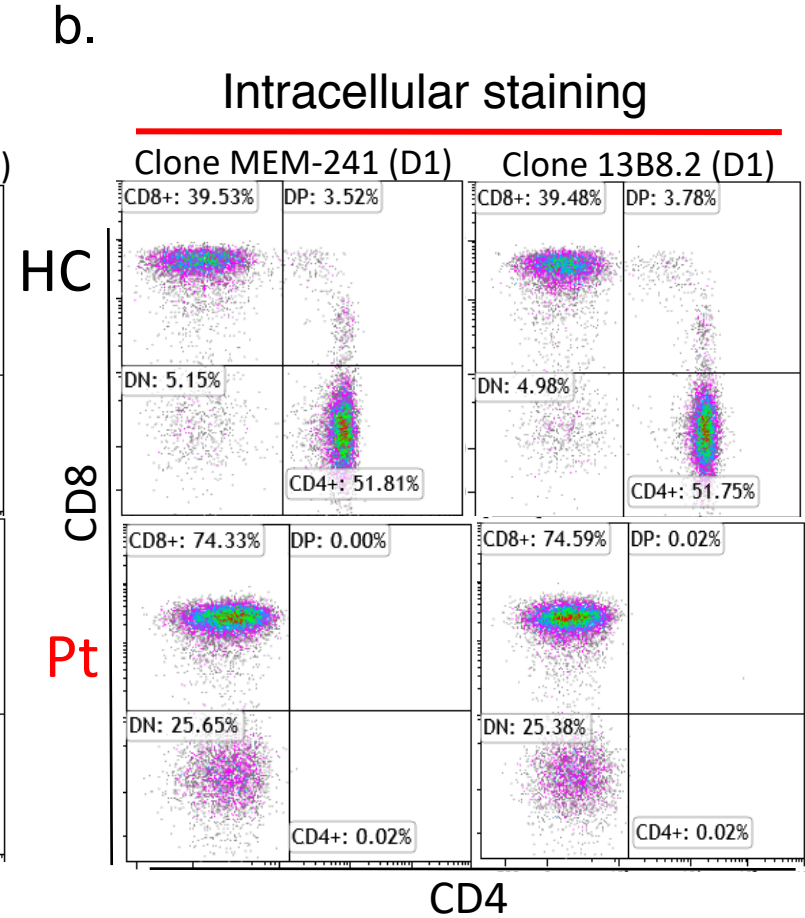
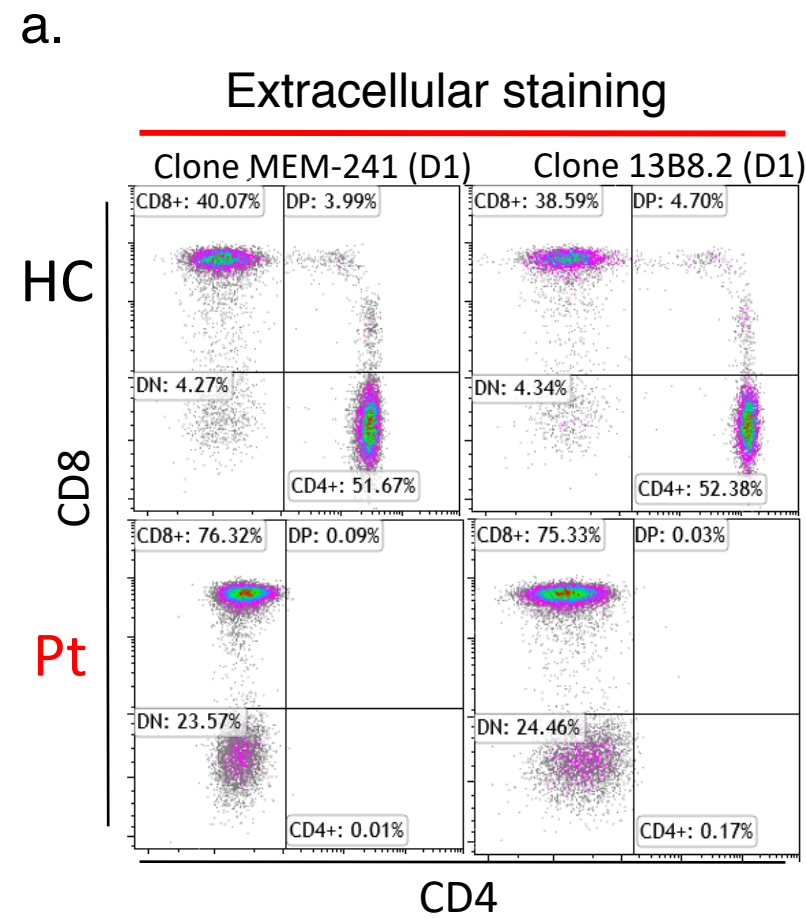
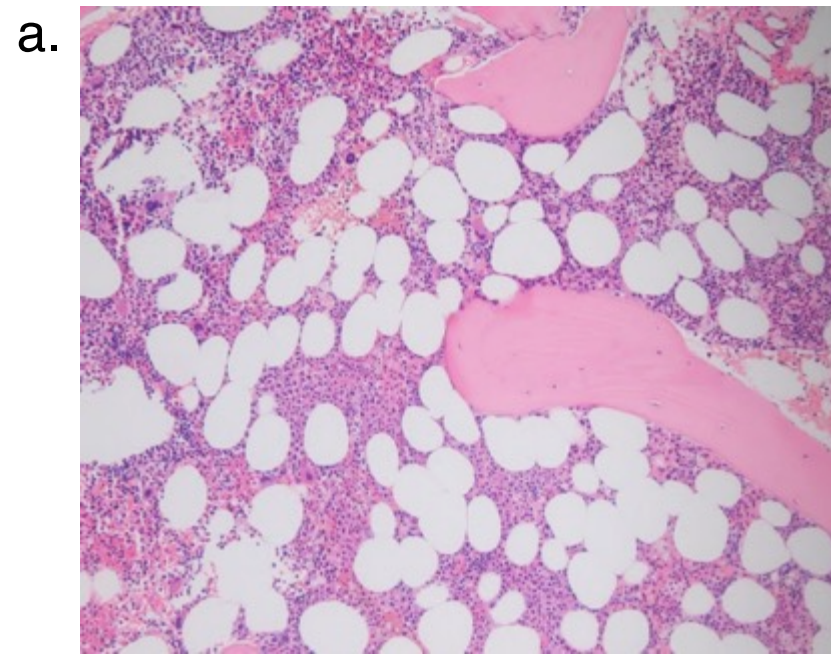


## **Supplementary Materials**

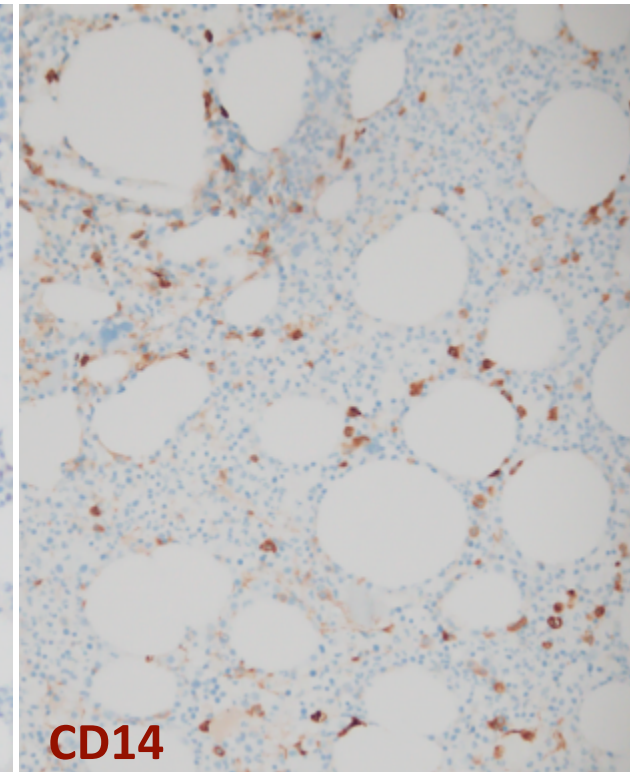
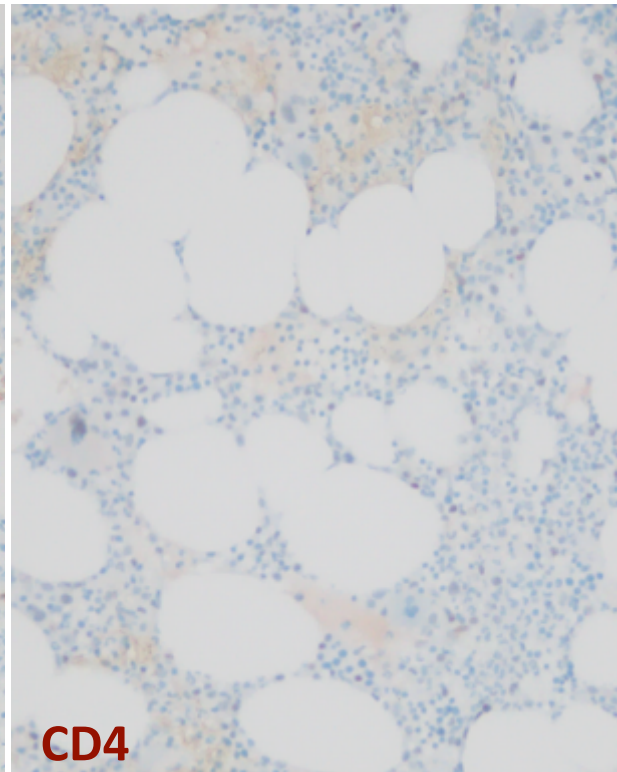
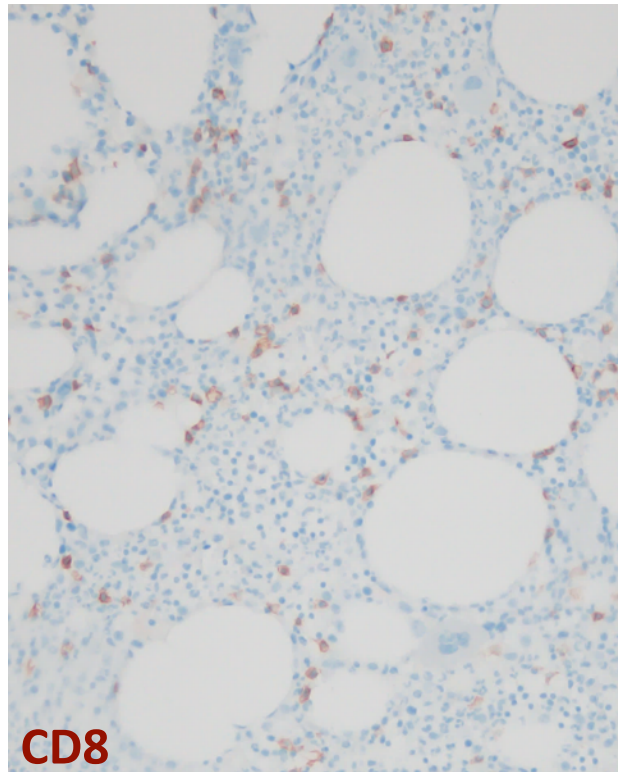
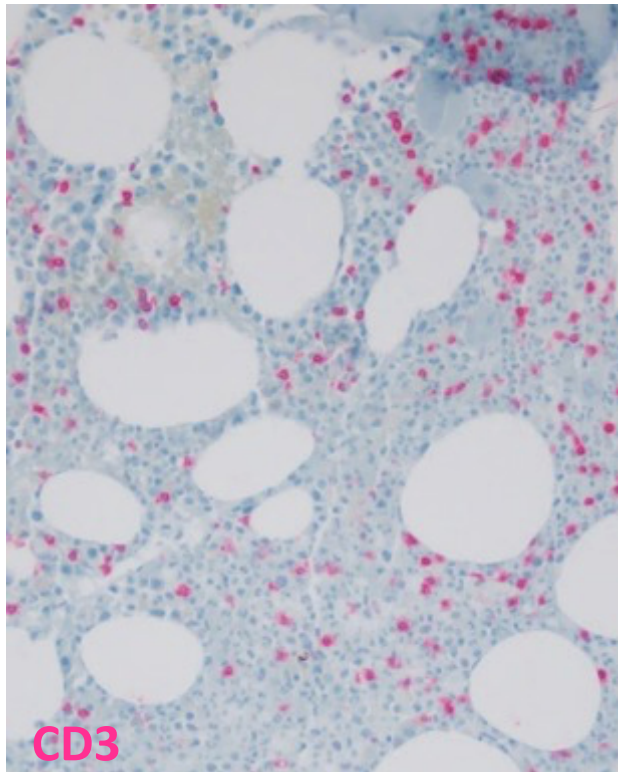
### **Lost in translation: Lack of CD4 expression due to a novel genetic defect**

- 1. Supplementary Figures**
- 2. Supplementary Figure Legends**
- 3. Supplementary Tables**
- 4. Supplementary Methods**
- 5. Supplementary Methods Table**
- 6. Supplementary Material References**



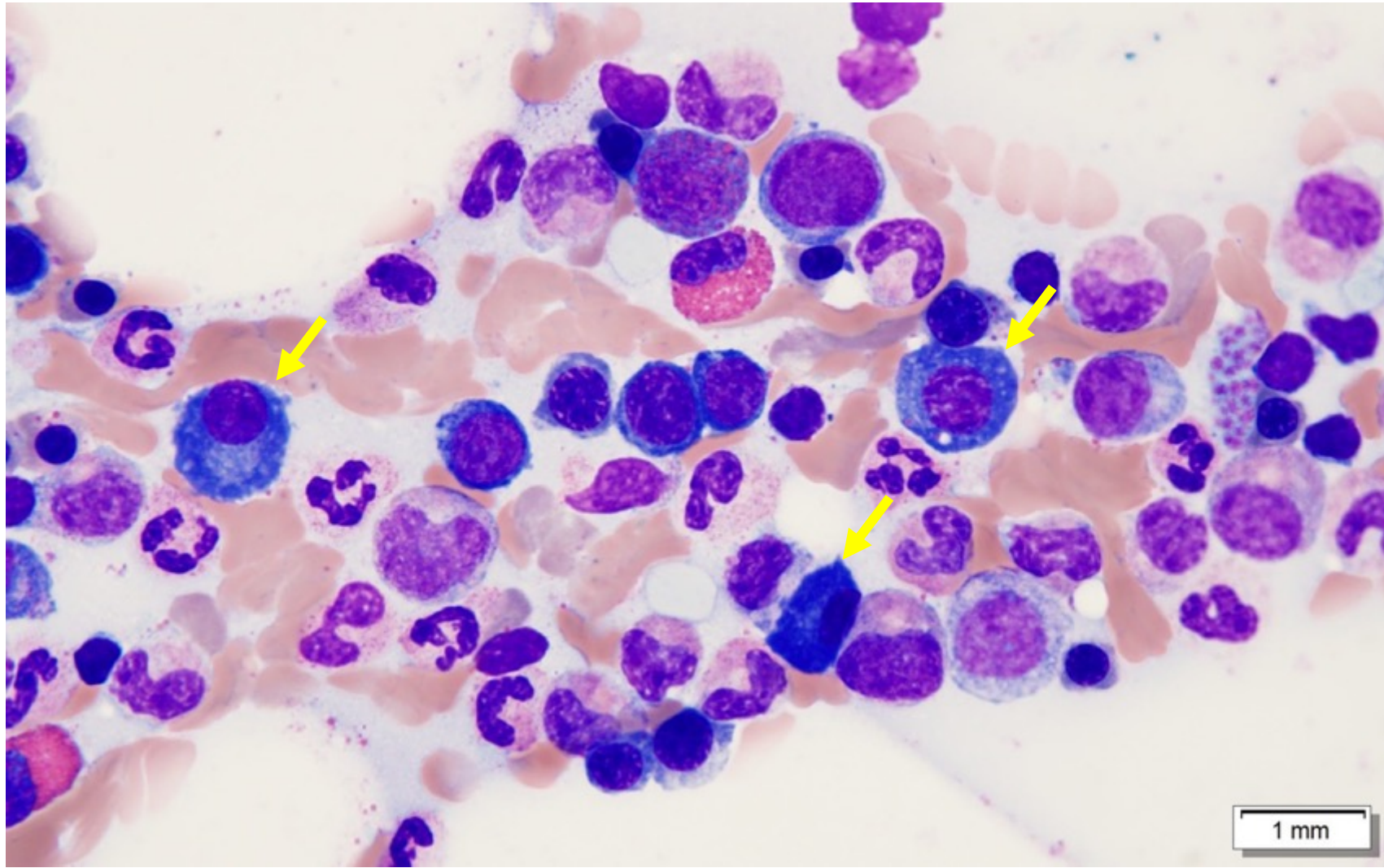


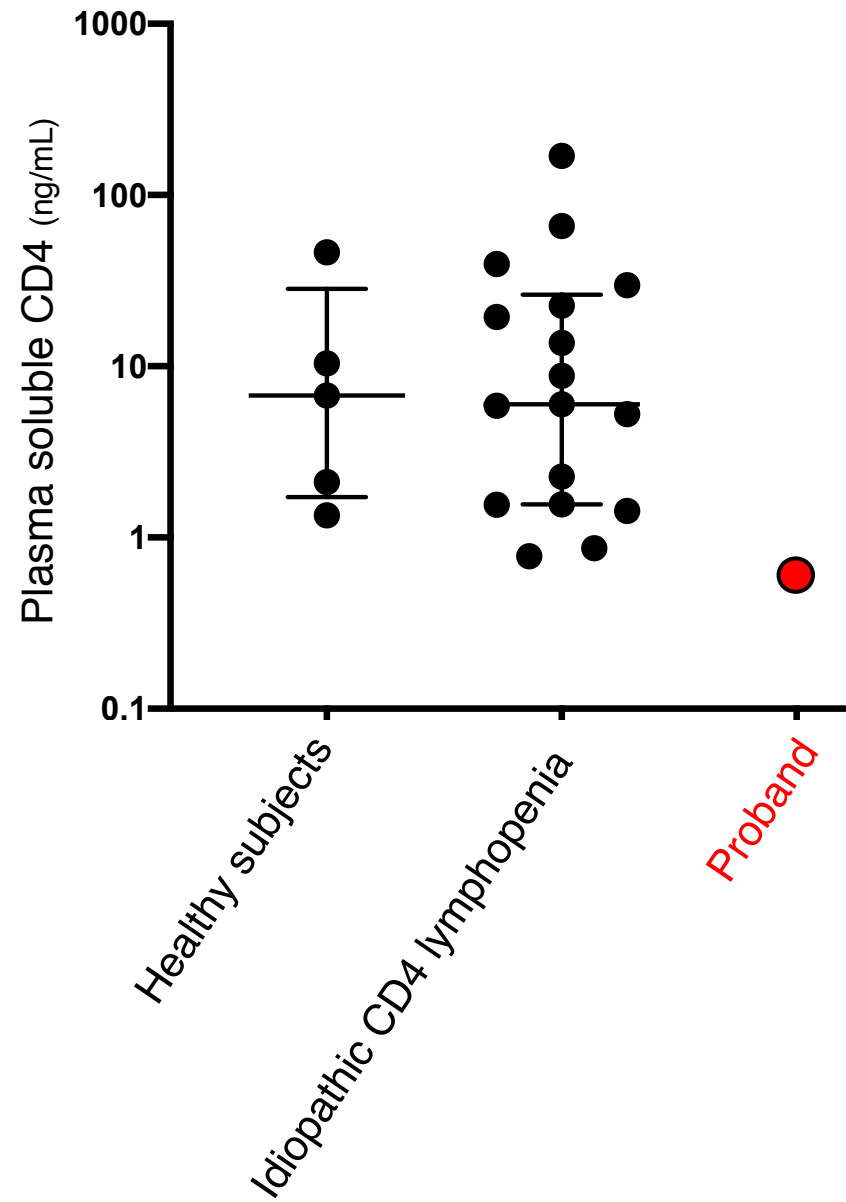
b.

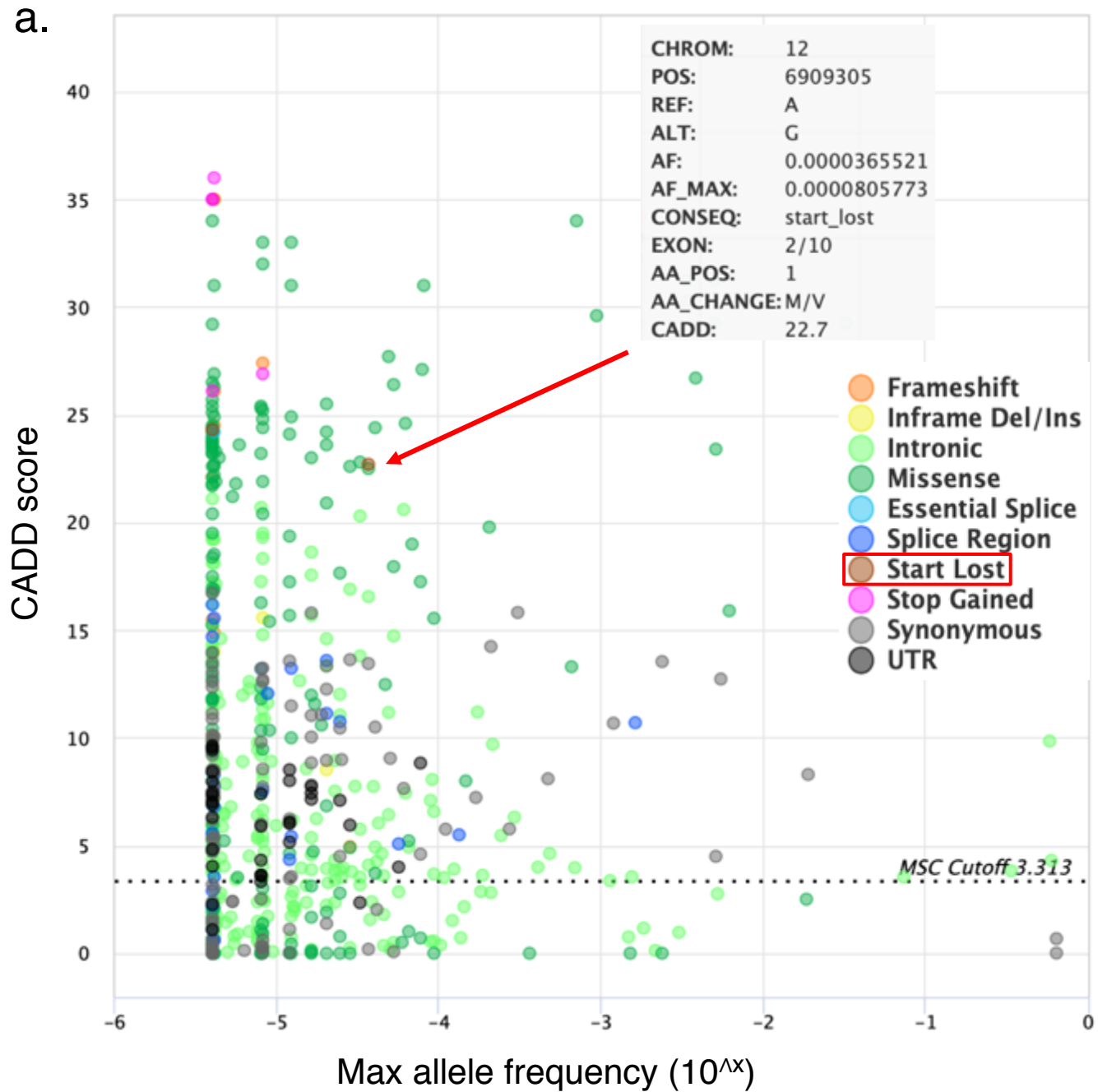




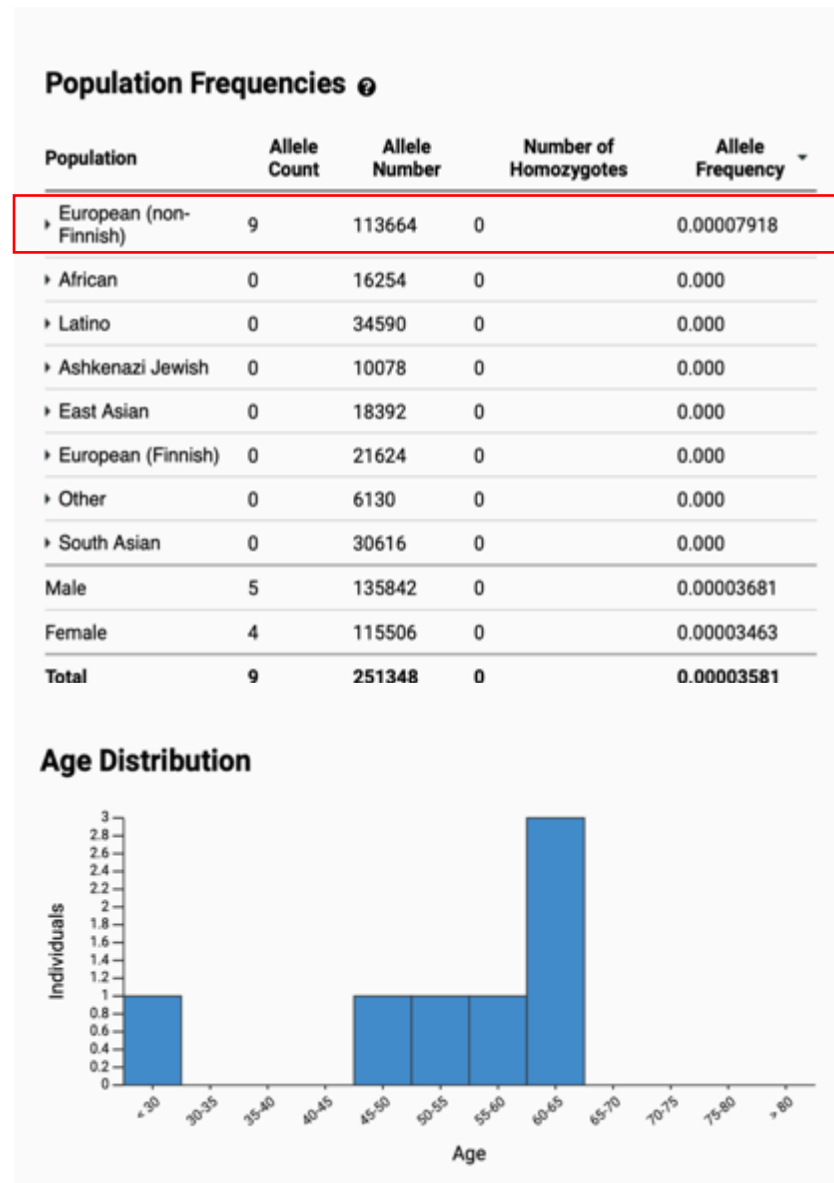
C.



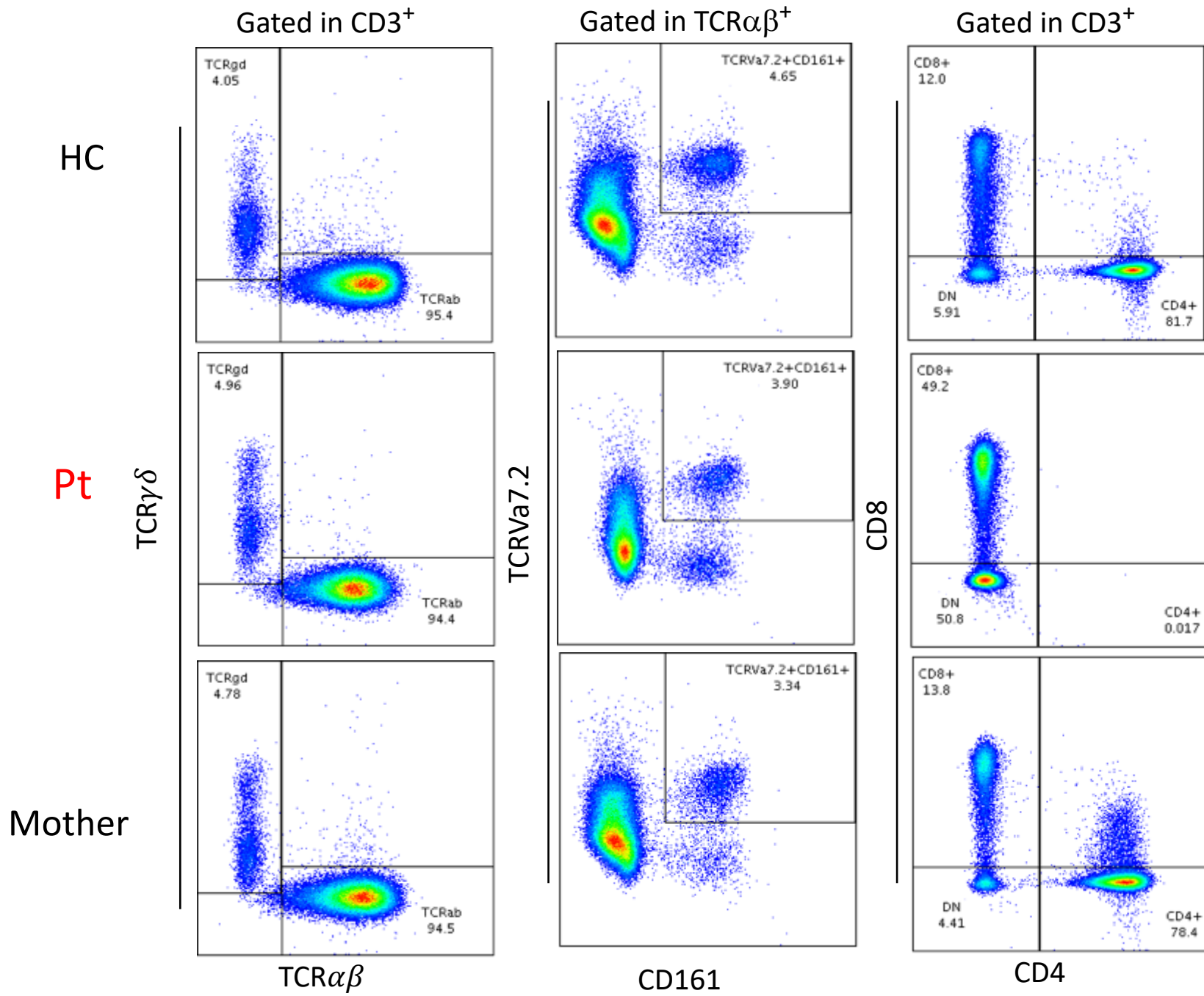




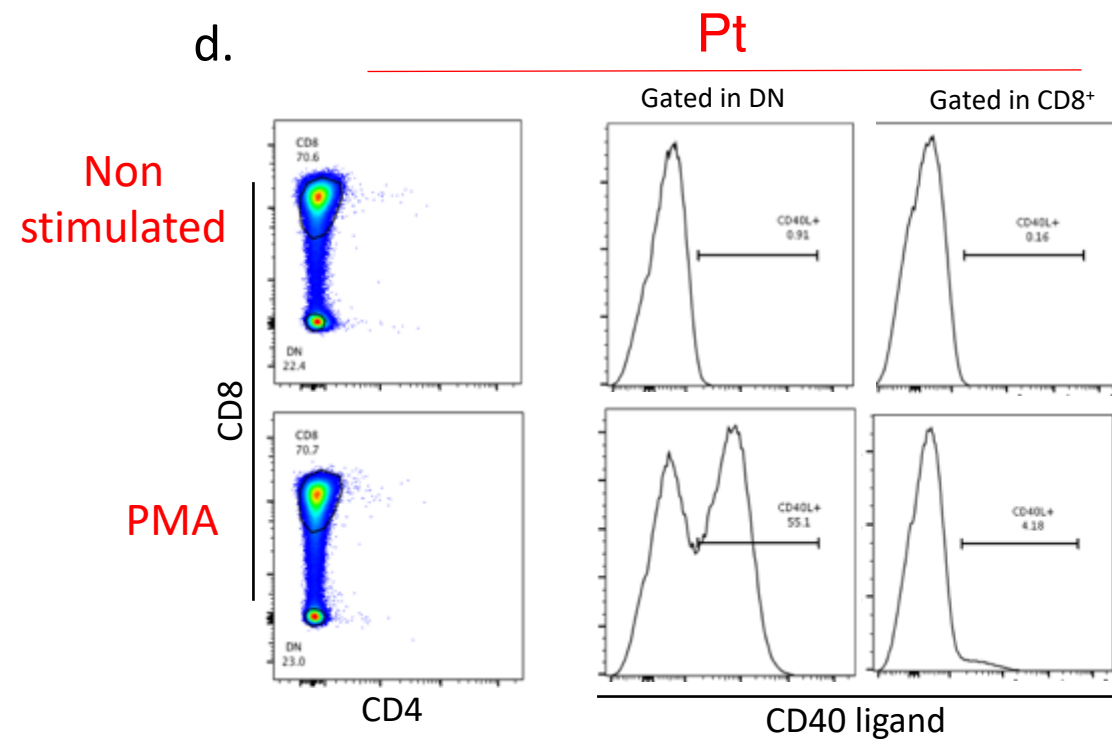
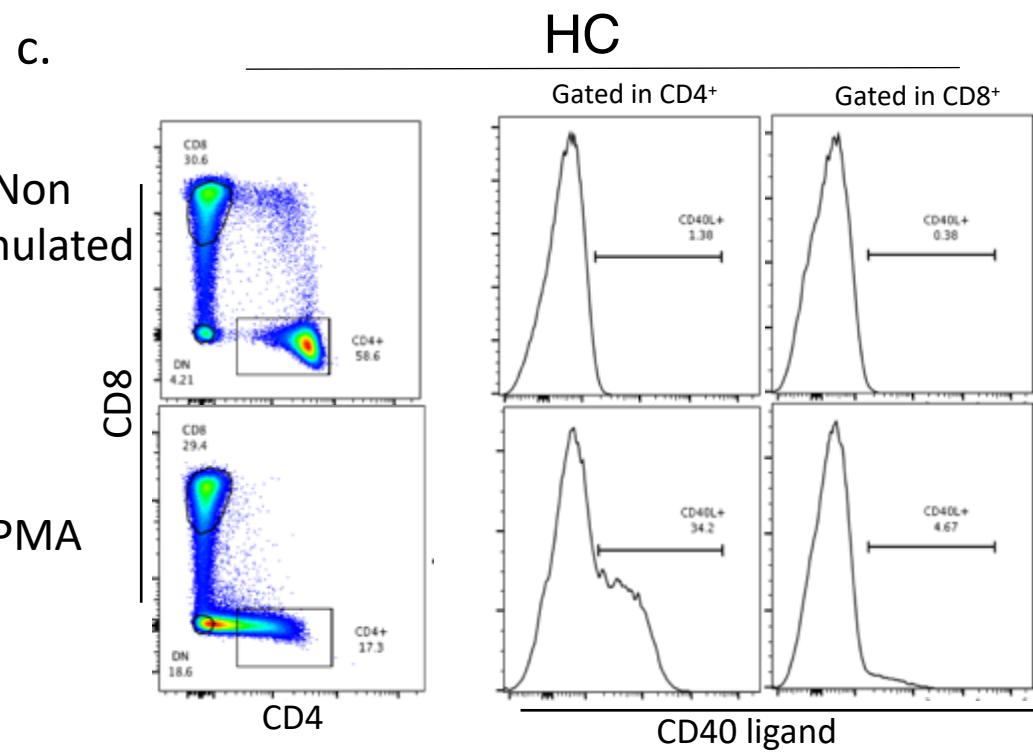
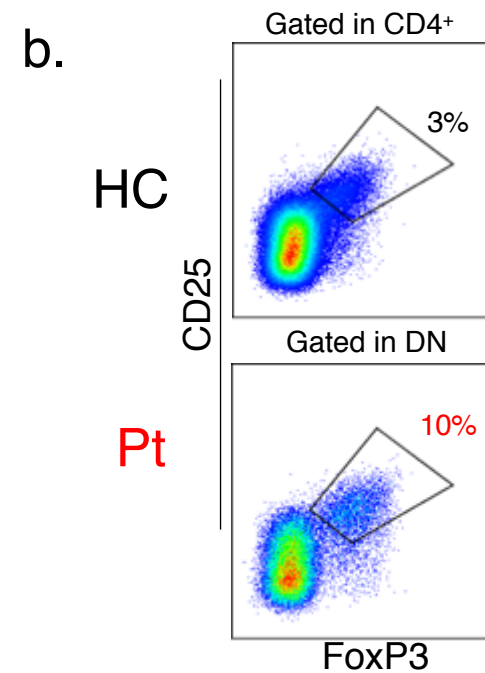
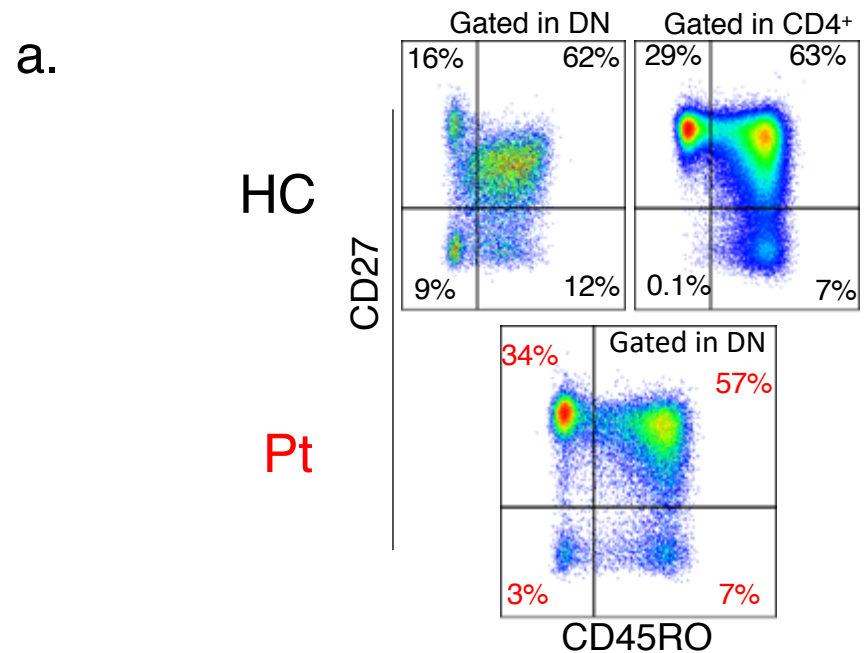
b.



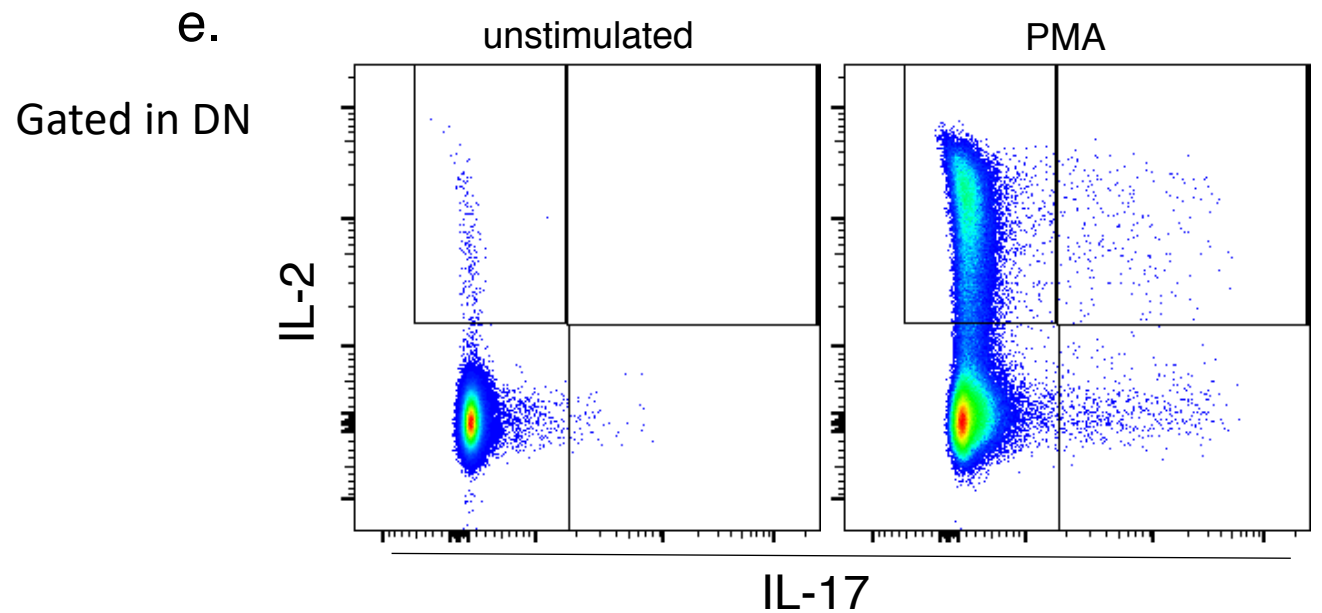
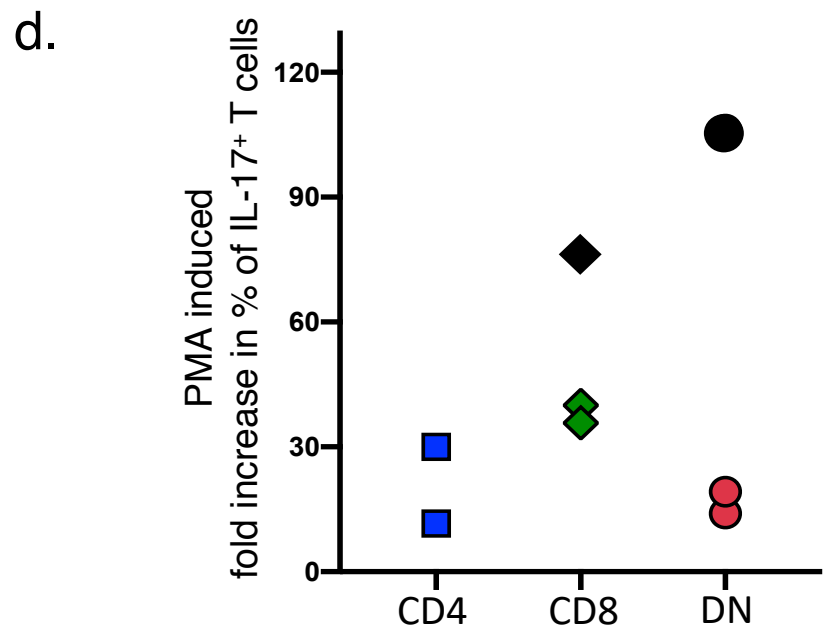
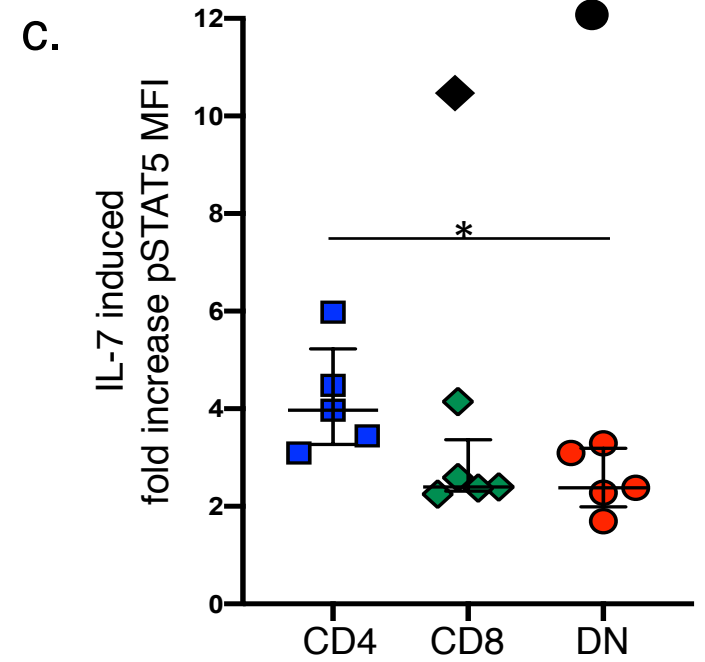
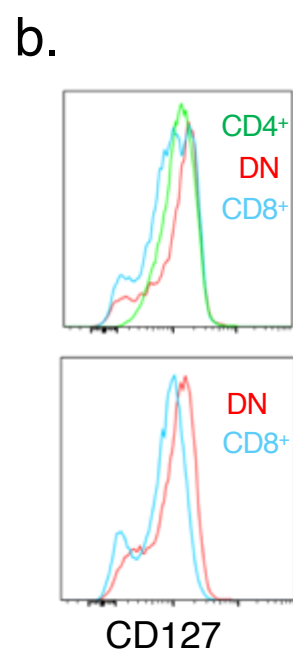
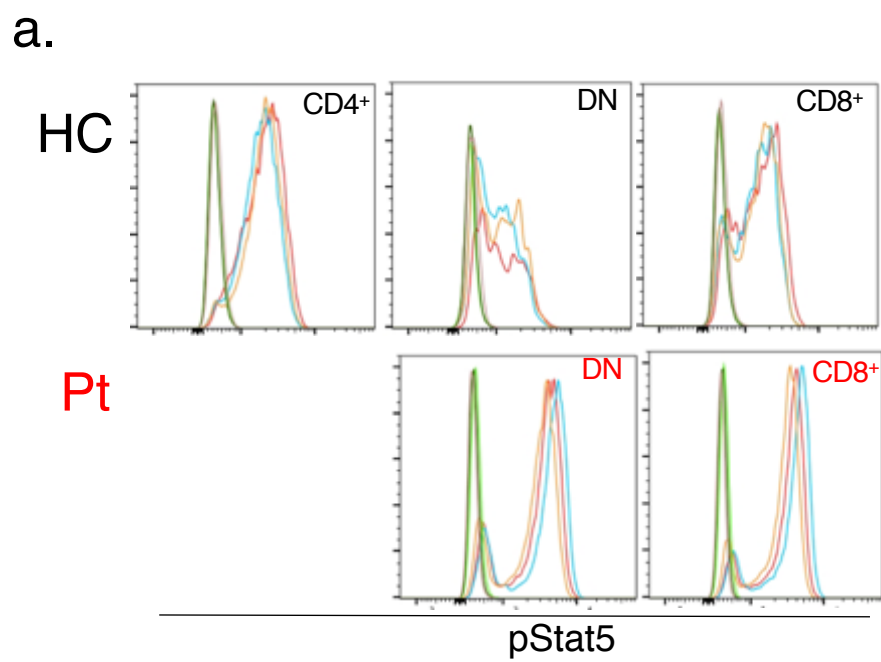
Supplementary Figure 4

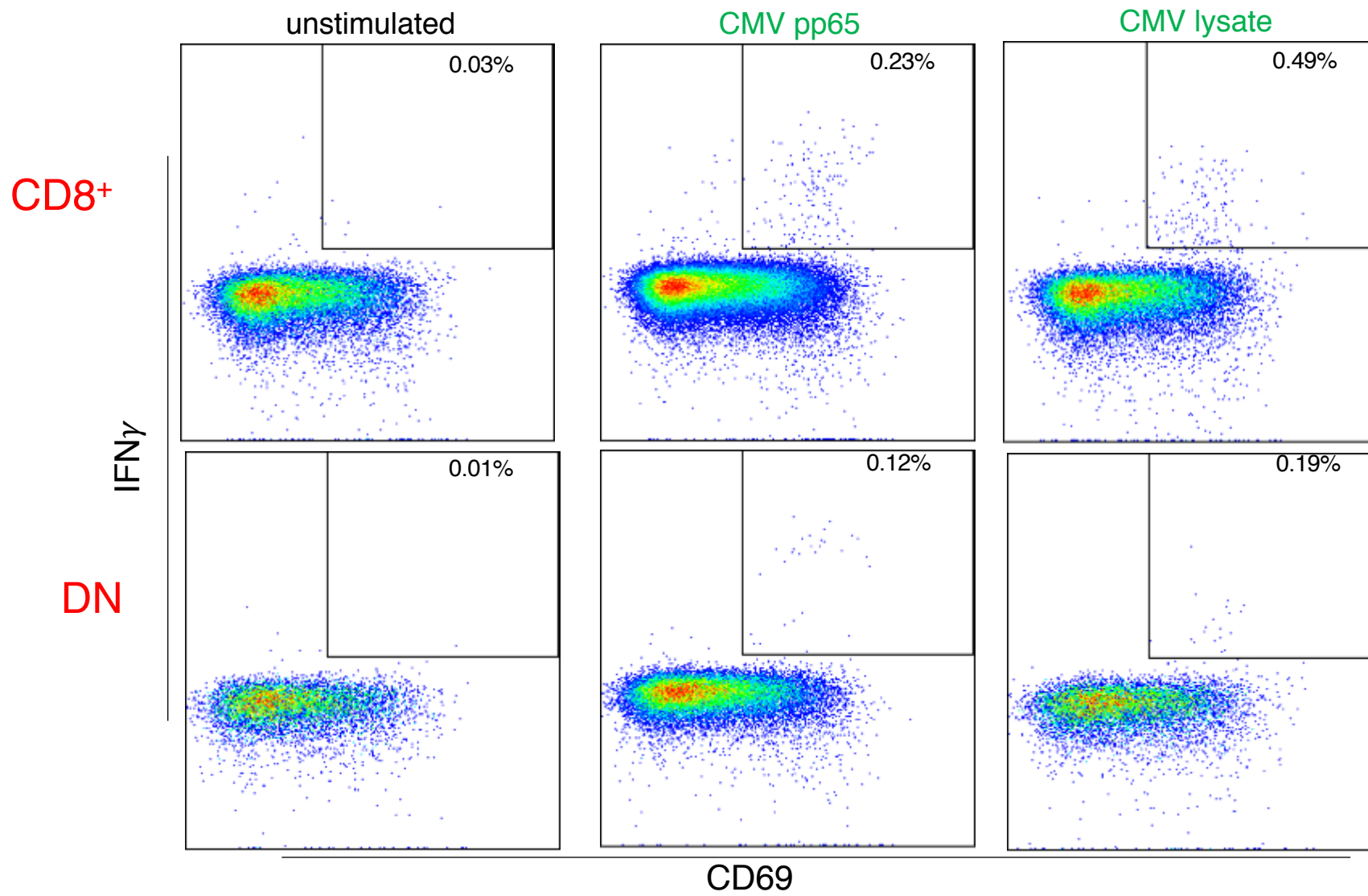


Supplementary Figure 5



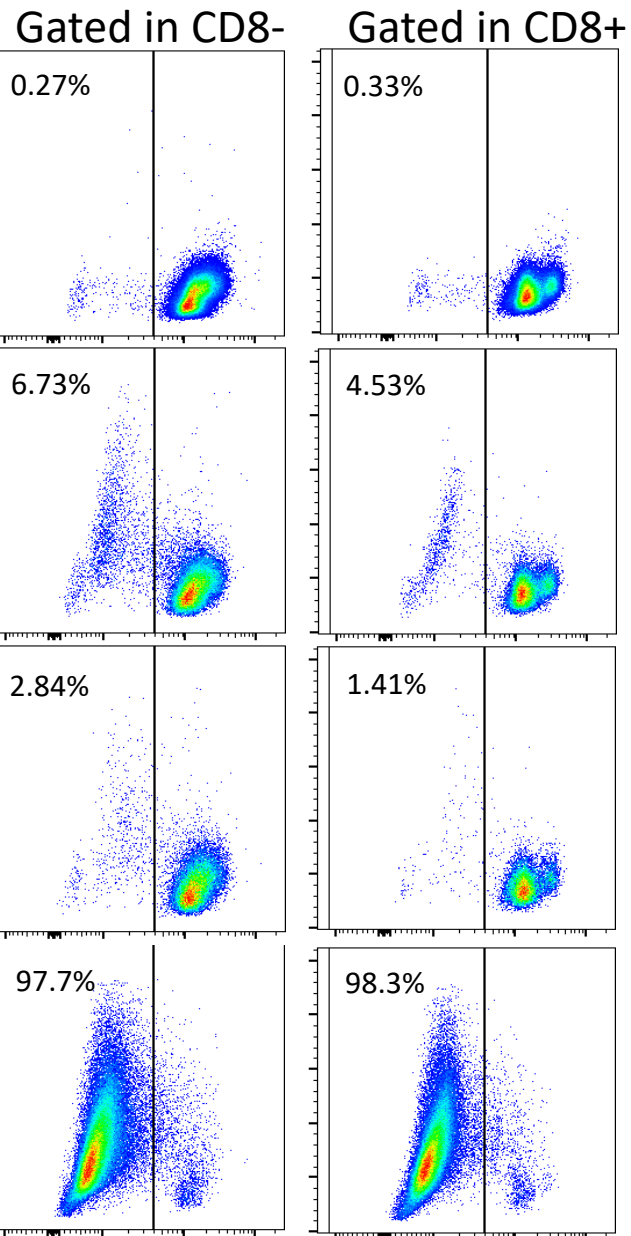




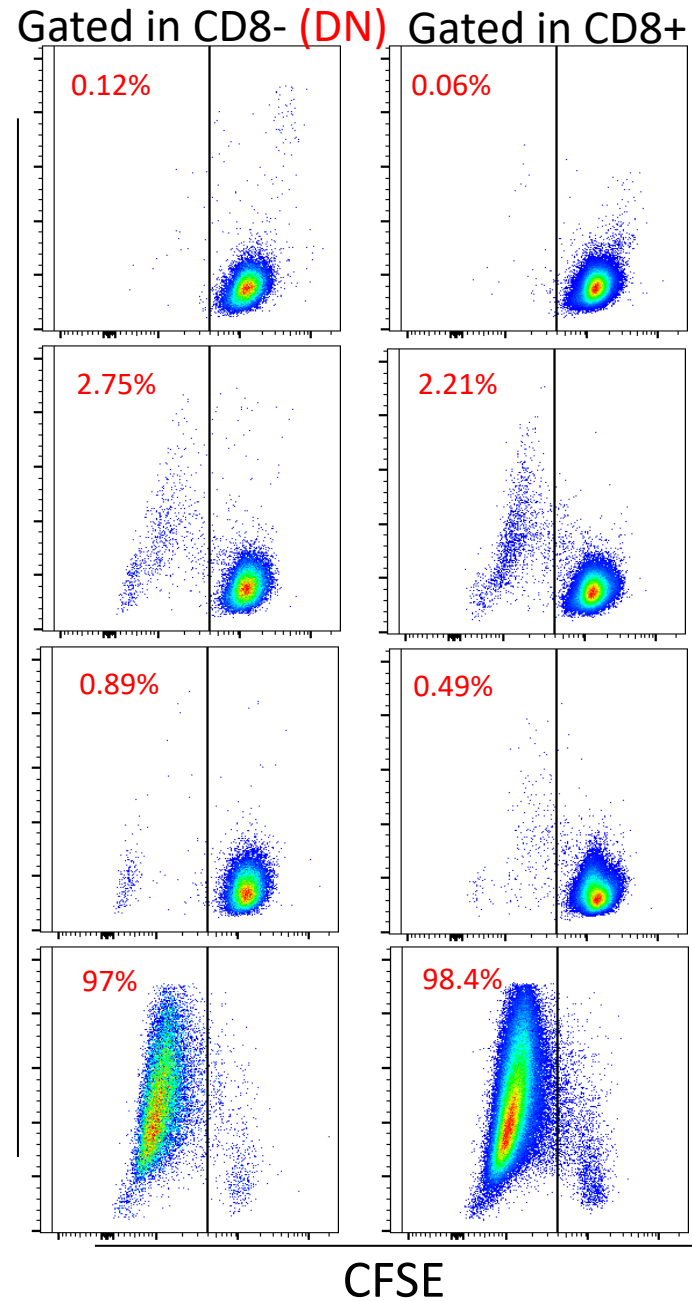


HC

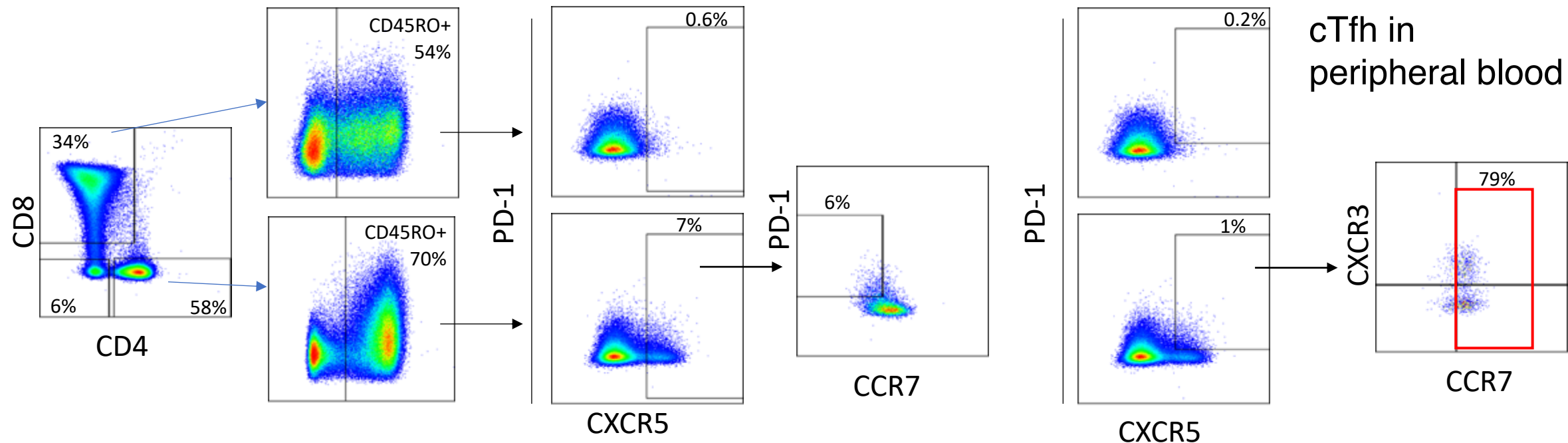
Unstimulated



Pt

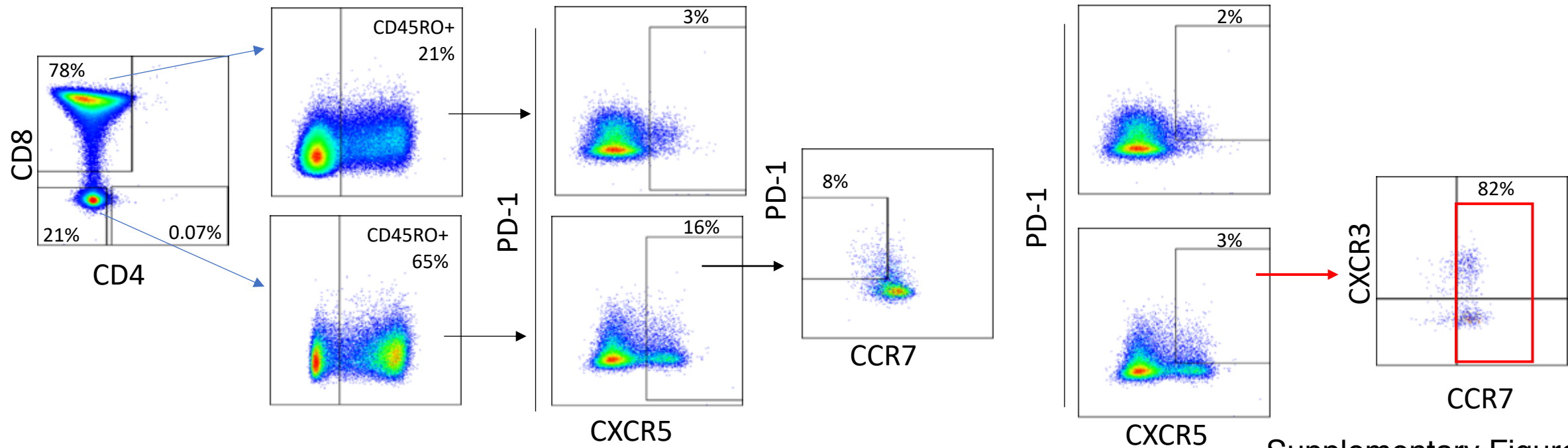


HC



cTfh in peripheral blood

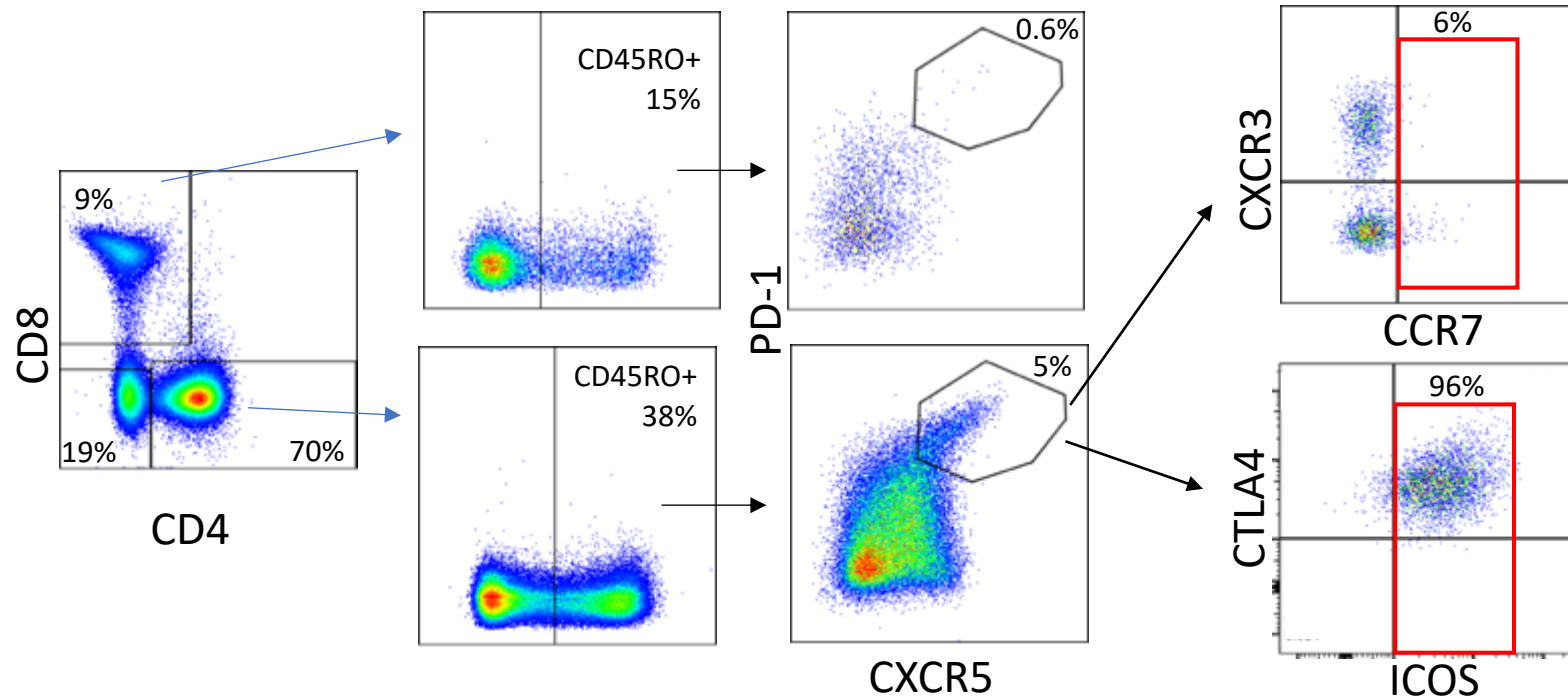
Pt



Supplementary Figure 10

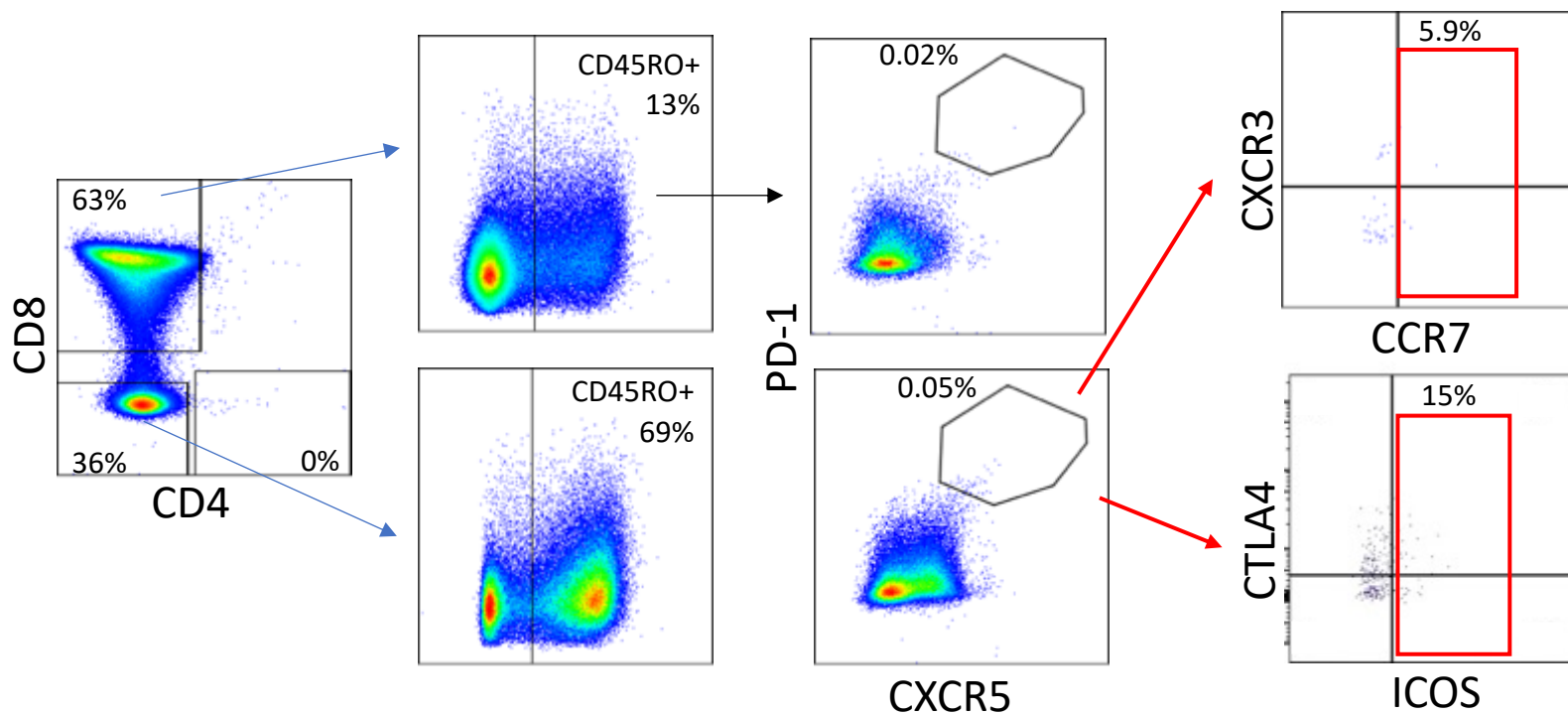


HC

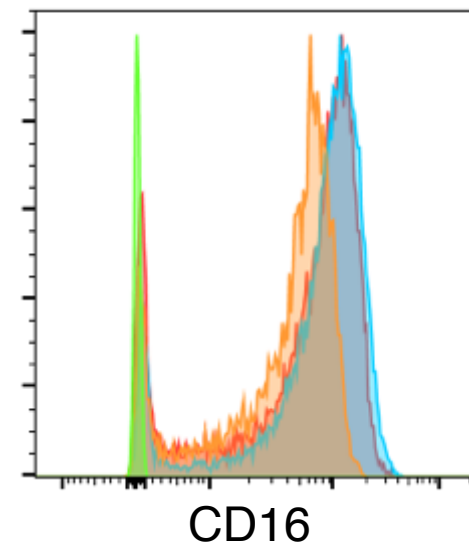
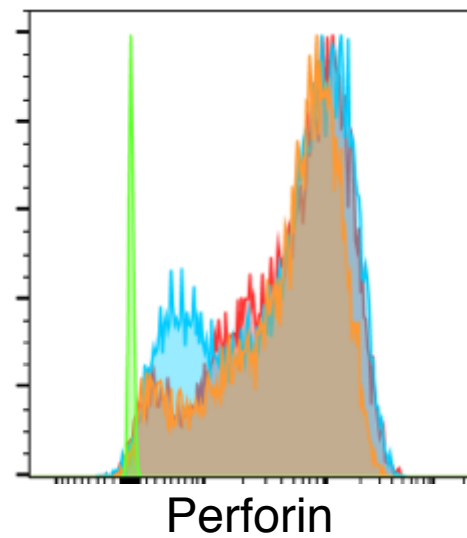
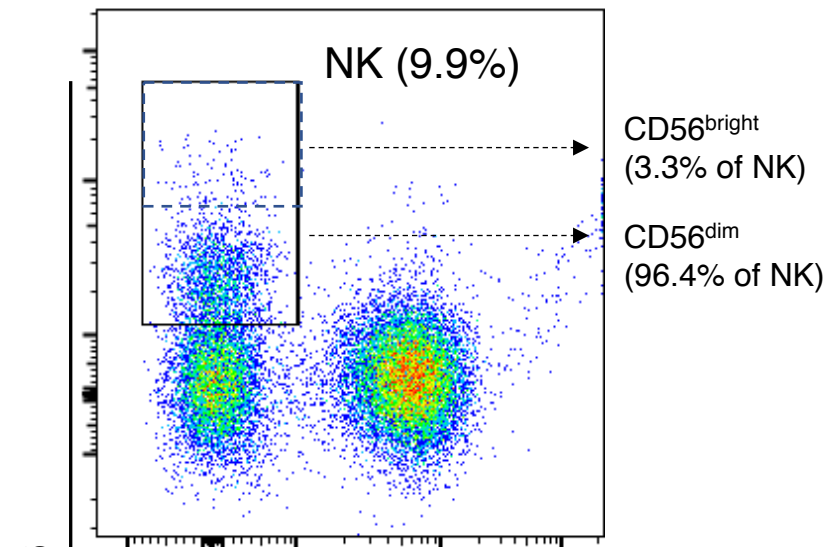


Tfh in lymph node

Pt

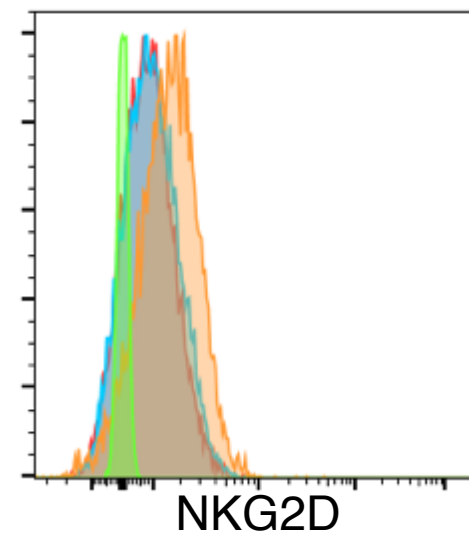
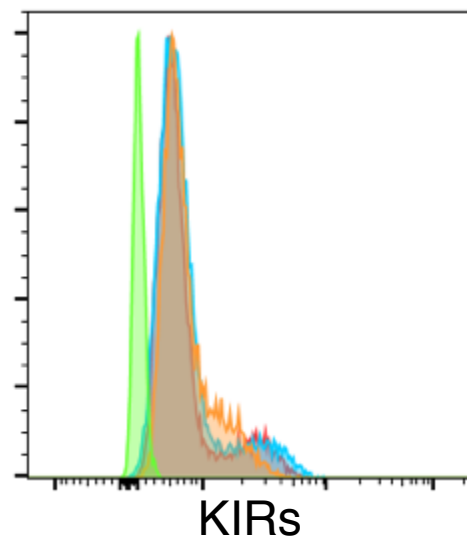
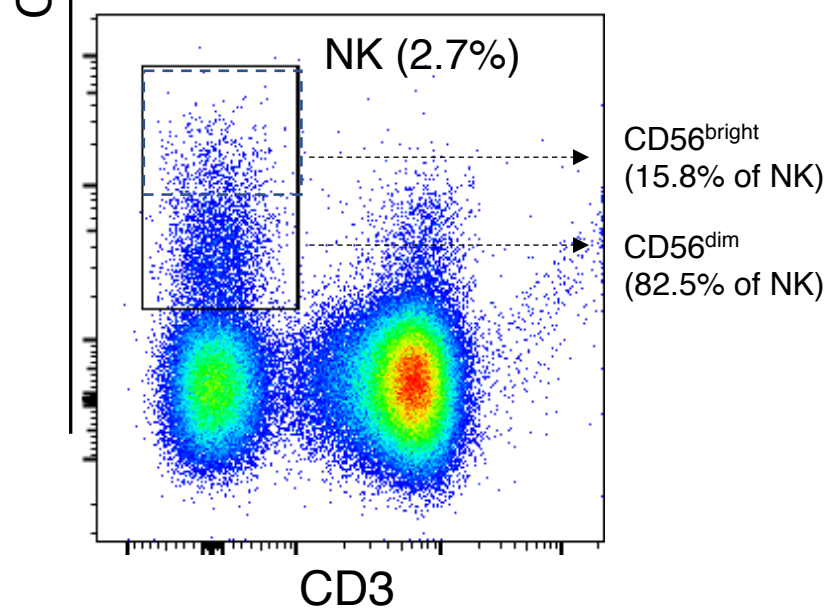


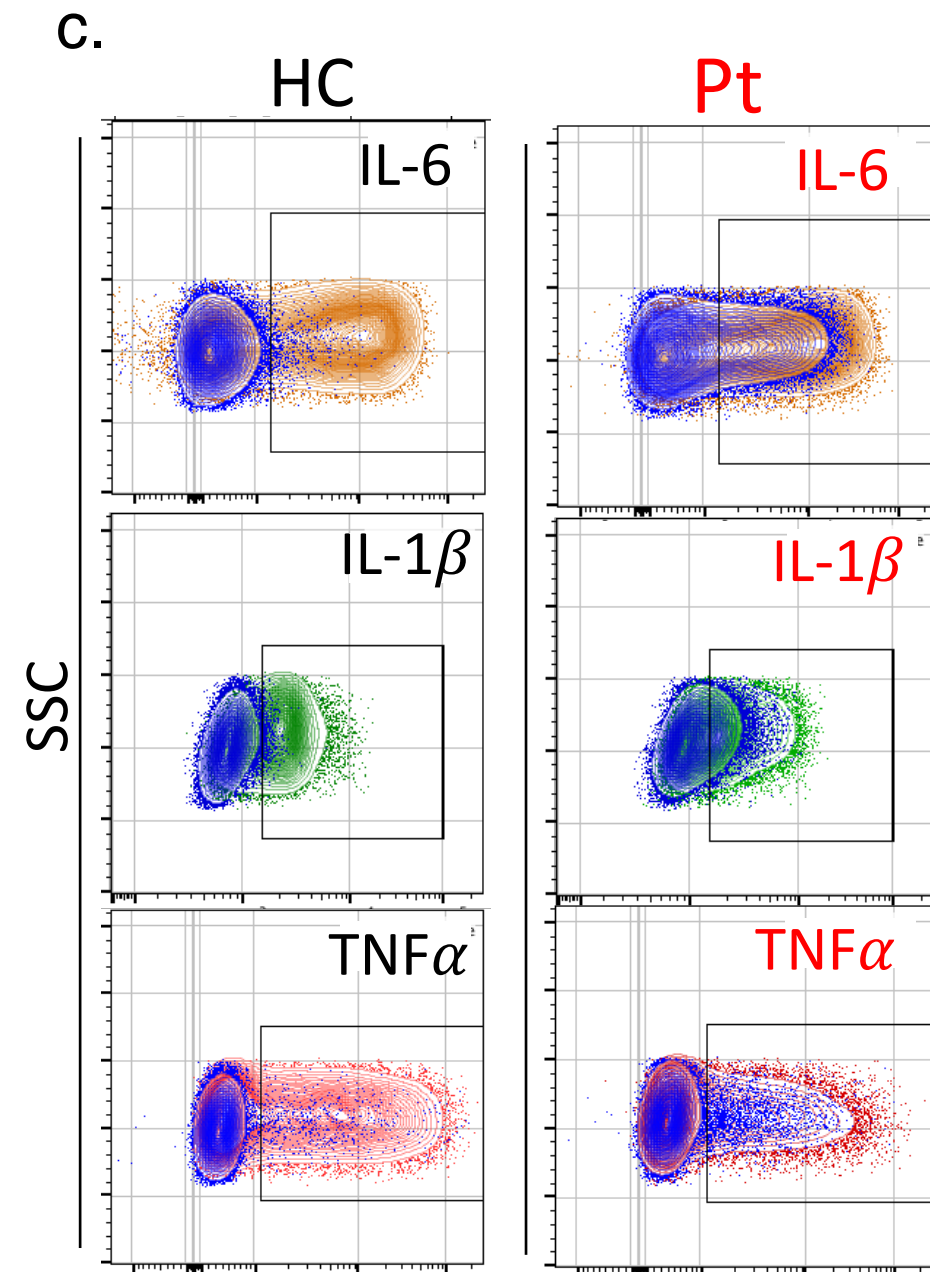
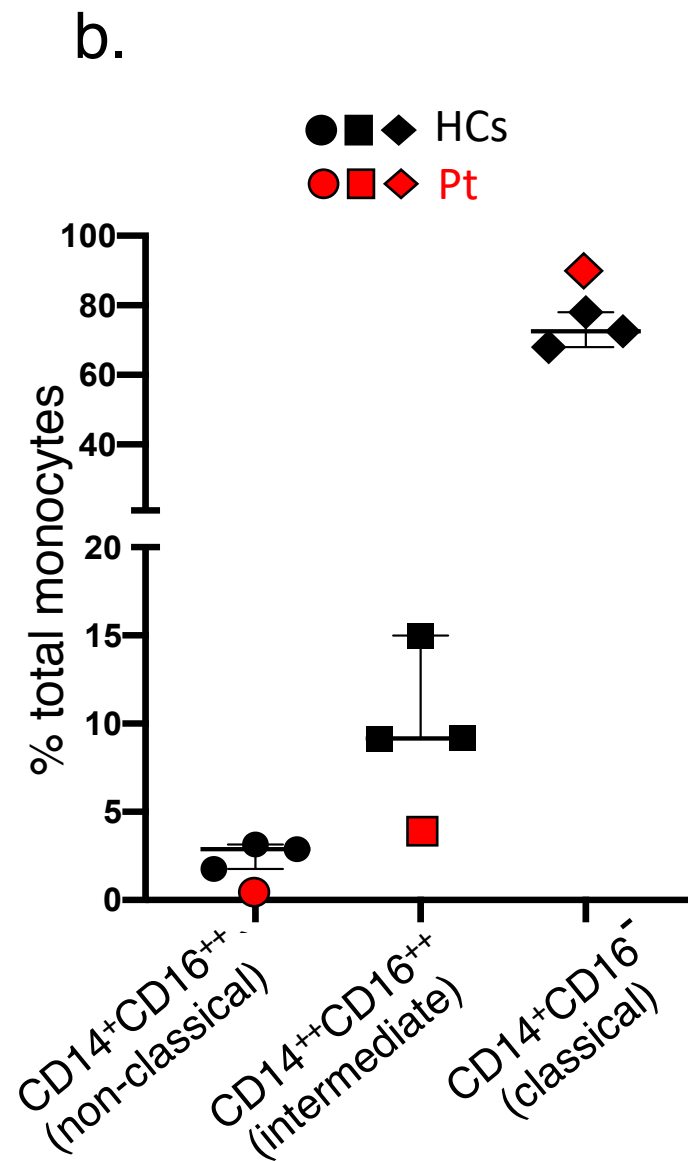
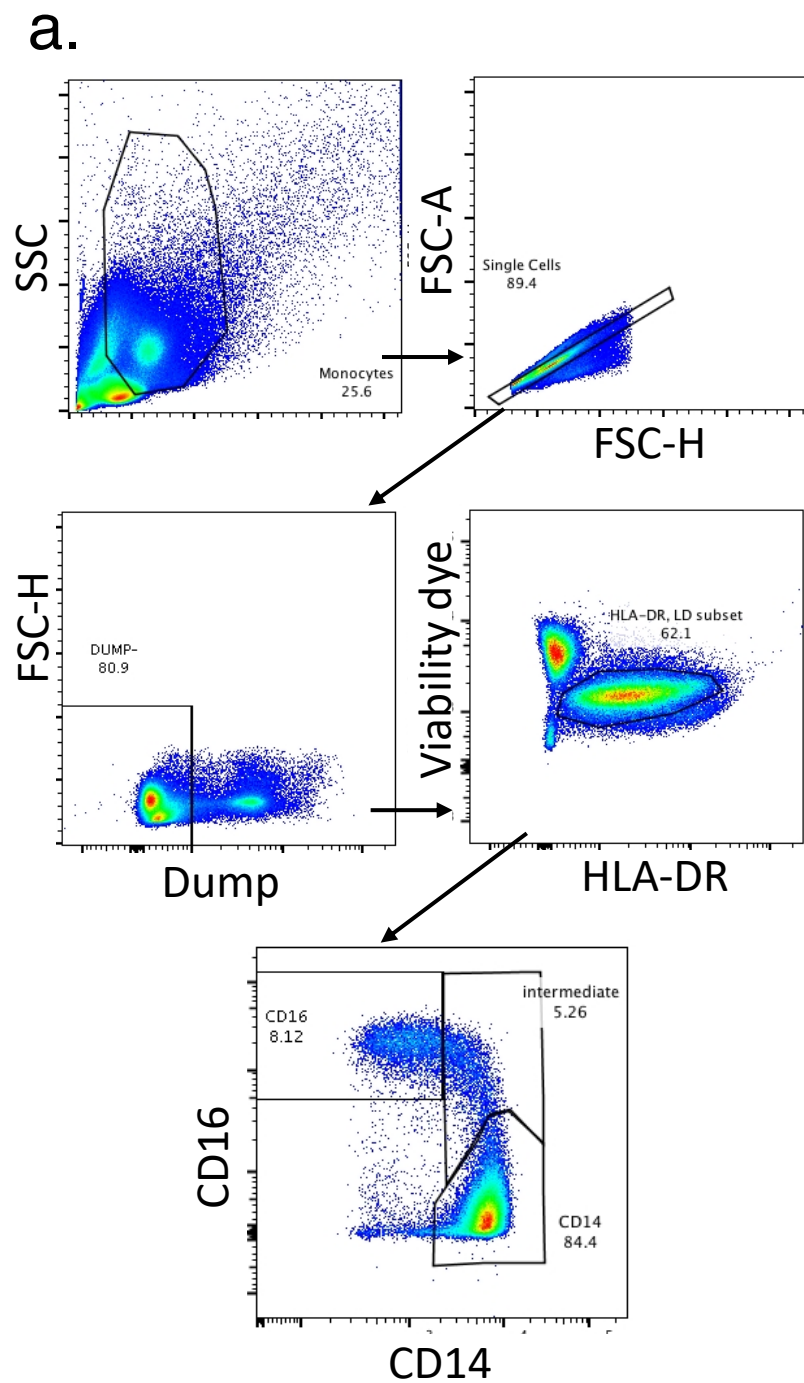
HC



Pt  
Mother  
HC  
Unstained

Pt

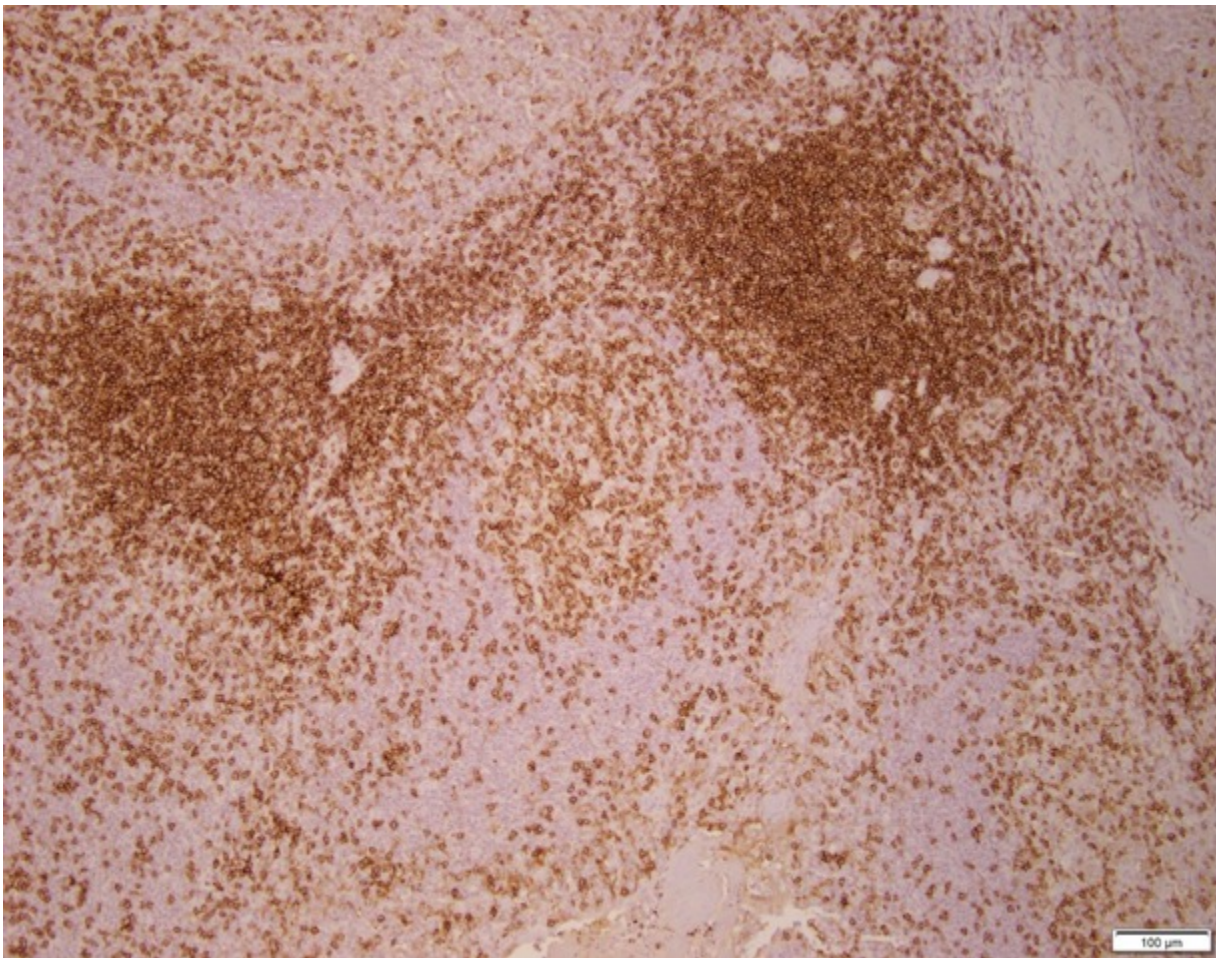




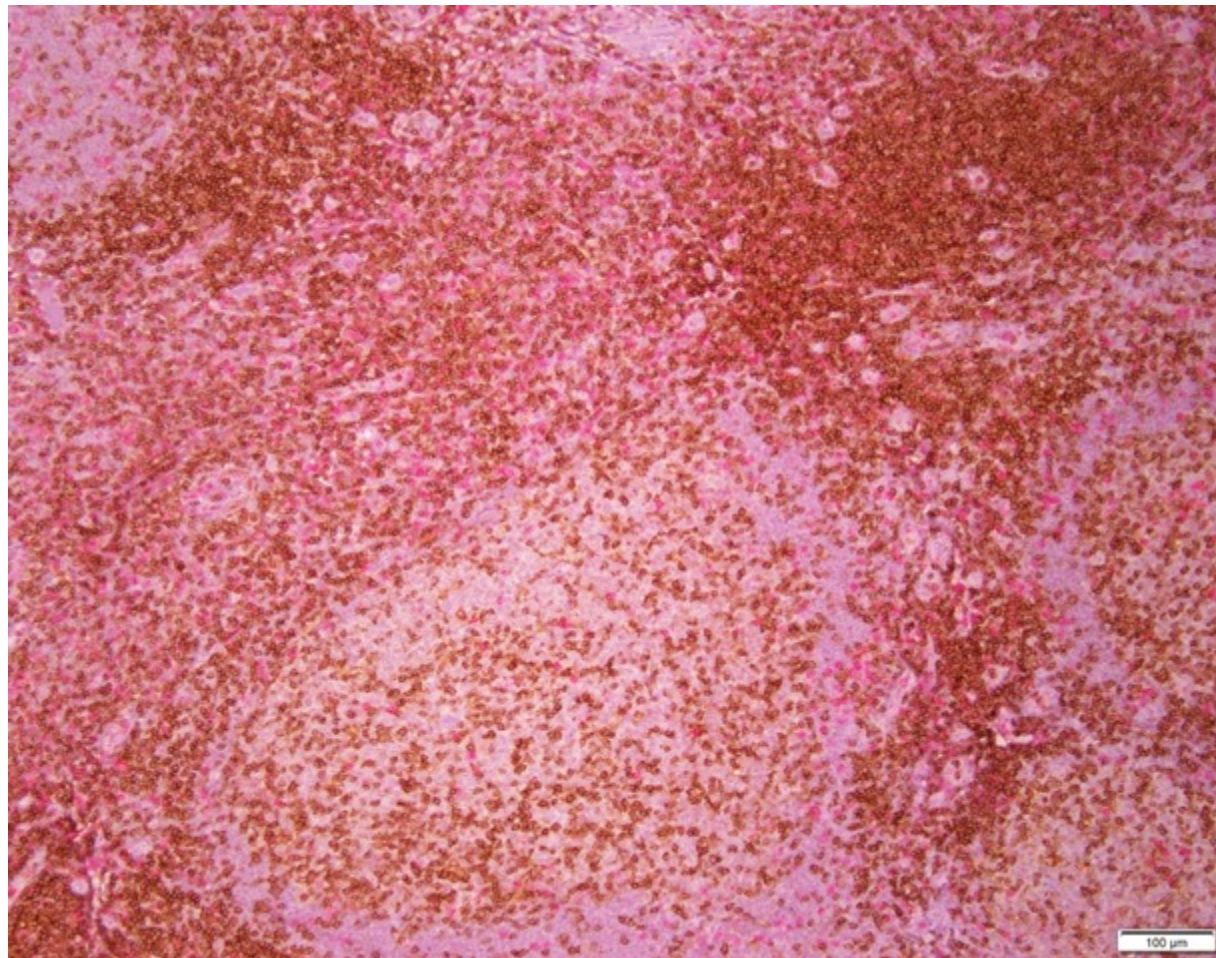
Supplementary Figure 13



a.



b.





## Supplementary Figures Legends:

### Supplementary Figure 1.

- a.** CD4 and CD8 T cells in healthy control (HC, upper panels) and in the proband (Pt, lower panels) using fluorescent-conjugated antibodies targeting different epitopes on the extracellular domains of CD4. For the flow cytometry analysis EDTA whole blood was used with the following antibodies: anti-human CD45 Krome Orange, anti-human CD3-PE, anti-human CD8 Pacific Blue, all from Beckman Coulter. For the CD4 analysis, 3 different clones were used, anti-human CD4 PC5 (clone 13B8.2), anti-human CD4 FITC (clone RPA-TA) and anti-human CD4 APC Cy7 (clone MEM241). Presented are results with MEM241 and 13B8.2 targeting D1 extracellular domain, similar results were obtained with RPA-TA.
- b.** CD4 and CD8 T cells in healthy control (HC, upper panels) and in the proband (Pt, lower panels) using fluorescent-conjugated antibodies targeting different epitopes on the extracellular domains of CD4 on permeabilized cells. PerFix-NC kit (Beckman Coulter) was used to permeabilize cells, 20,000 CD45<sup>+</sup> lymphocyte events were collected on a CytoFlex® flow cytometer (Beckman Coulter) and the data were analyzed with Kaluza C software, v1.2 (Beckman Coulter).
- c.** Distribution of fluorescence intensity of CD4 staining in non-permeabilized and permeabilized monocytes from a healthy control (HC, cyan histogram), proband (Pt, red histogram) and isotype control (grey histogram) using a fluorescent-conjugated antibody targeting the D3 extracellular domain of CD4 (clone SK3).

### Supplementary Figure 2.

- a.** Hematoxylin/eosin staining of a bone marrow core biopsy showing a normocellular marrow for age (70%) with maturing trilineage hematopoiesis.
- b.** Immunohistochemical staining of the bone marrow core biopsy: total T cells are highlighted by the CD3 staining (red), while CD8 (brown) highlights a subset of T cells. CD4 staining is negative (both, T cells and monocytes are negative for CD4). CD14 highlights monocytes, adequate in number, dispersed throughout the medullary cavity.
- c.** Bone marrow aspirate stained with modified Giemsa shows a normal proportion and distribution of plasma cells (yellow arrows).

### Supplementary Figure 3.

Plasma levels of soluble CD4 as measured by ELISA in healthy subjects (HC, n=5), patients with Idiopathic CD4 lymphopenia (ICL, n=17, median CD4: 107 cells/ $\mu$ L) and proband. Presented is the median and 25-75<sup>th</sup> interquartile range for HC and ICL subjects.

### Supplementary Figure 4.

- a. Visualization of allele frequency and mutation damage prediction scores of all reported CD4 *gene* variants [1]. Red arrow indicates the c.1A>G variant.
- b. Population frequency and age distribution of c.1A>G in gnomAD.

### Supplemental Figure 5.

Mucosal-associated invariant T (MAIT)-cells were identified as lymphocytes expressing CD3, TCR $\alpha\beta$ , CD161 and TCR V $\alpha$ 7.2 in peripheral blood from a healthy subject (HC, upper panel), proband (Pt, mid panel) and proband's mother (lower panel). Despite the loss of CD4 expression on T cells (right panel), MAIT-cells were preserved in peripheral blood of the proband.

### Supplemental Figure 6.

- a. Distribution of naïve (CD45RO<sup>-</sup>CD27<sup>+</sup>) and memory (CD45RO<sup>+</sup>CD27<sup>+</sup>; CD45RO<sup>+</sup>CD27<sup>-</sup>; CD45RO<sup>-</sup>CD27<sup>+</sup>) T-cells subsets in CD4<sup>-</sup>CD8<sup>-</sup> double negative (DN) from healthy control (left upper panel), in CD4<sup>+</sup> from healthy subject (right upper panel) and in the CD4<sup>-</sup>CD8<sup>-</sup> DN from the proband (lower panel).
- b. Distribution of regulatory T-cells (CD25<sup>+</sup>FOXP3<sup>+</sup>) in CD4<sup>+</sup> T-cells from a healthy control (upper panel) and in the CD4<sup>-</sup>CD8<sup>-</sup> DN T-cells from the proband (lower panel).
- c. Expression of CD40-Ligand in unstimulated and PMA-stimulated CD4<sup>+</sup> and CD8<sup>+</sup> T-cells subsets in an healthy control subject.
- d. Expression of CD40-Ligand in unstimulated and PMA-stimulated DN and CD8<sup>+</sup> T-cells subsets in the proband.

### Supplementary Figure 7.

- a. IL-7 signaling evaluation by phosphorylated STAT5 staining after IL-7 stimulation in CD4<sup>+</sup>, DN and CD8<sup>+</sup> T-cells from a healthy control (upper panels) and DN and CD8<sup>+</sup> T-

cells from the proband (lower panel). Green and grey histograms represent unstimulated condition and isotype staining control, while cyan, red and yellow histograms represent 3 replicates of IL-7 stimulation at 10 ng/mL.

- b.** Distribution of fluorescence intensity of CD127 staining in T-cell subsets from a healthy control (upper panel) and proband (lower panel). Green, red and cyan histograms represent the distribution of CD127 expression in CD4<sup>+</sup>, DN and CD8<sup>+</sup> T-cells, respectively.
- c.** Phosphorylation of STAT5 in response to IL-7 stimulation (10 ng/mL) expressed as mean fluorescence intensity (MFI) fold increase compared to unstimulated sample. The response in CD4, CD8 and DN T cell subsets from 4 different HCs (blue square, green diamond and red circles, respectively) and in proband's CD8 and DN T cells (black diamond and circles) is presented. The median and 25-75% interquartile range of the MFI of HCs are presented. Note that a statistically significant higher pSTAT5 in CD4 compared to DN is observed in HCs.
- d.** Intracellular detection of IL-17 in response to PMA stimulation is presented in CD4, CD8 and DN T cell subsets from 2 different HCs (blue square, green diamond and red circles, respectively) and in proband's CD8 and DN T cells (black diamond and circles).
- e.** Intracellular detection of IL-2 and IL-17 in proband's DN T cells in resting conditions (left panel) and upon PMA stimulation (right panel).

### **Supplementary Figure 8.**

Evaluation of CMV-specific T-cell responses by assessing the proband's activated (CD69<sup>+</sup>)-IFN $\gamma$  producing CD8<sup>+</sup> T-cells (upper panels) and DN T-cells (lower panels) in unstimulated experimental condition (left panels), upon CMV pp65 stimulation (central panels) and upon stimulation with CMV viral lysate (right panels).

### **Supplementary Figure 9.**

The proliferative response in different T cell subsets and experimental conditions in a one-way mixed lymphocyte reaction is presented. Monocytes from the same allogeneic stimulator have been co-cultured with CD3<sup>+</sup> T cells from a HC (left panels) and proband (right panels). Proliferative responses in T cell subsets upon 6 days of co-culture with allogeneic monocytes have been measured by CFSE dilution by gating in an healthy subject CD8<sup>+</sup> and CD8<sup>-</sup> T cells

(constituted by 95% CD4<sup>+</sup> T cells) and proband's CD8<sup>+</sup> and CD8<sup>-</sup> T cells (constituted by DN T cells). The 4 different experimental conditions are designated as 'unstimulated' indicating culture of CD3<sup>+</sup> T cells in absence of allogenic monocytes, 'MLR' designating the mixed lymphocyte reaction with co-culture with allogenic monocytes, 'MLR +  $\alpha$ MHCII' in which the allogenic monocytes are pre-incubated with an MHCII blocking antibody and ' $\alpha$ CD3 +  $\alpha$ CD28' in which HC or proband's T cells are stimulated with a CD3 and CD28 cross-linking antibody.

#### **Supplementary Figure 10.**

Gating strategy for the identification of T-cells expressing phenotypic markers specific for circulating Tfh (CXCR5 and PD-1) within the CD4, CD8 or DN T CD45RO<sup>+</sup> subsets in peripheral blood of a healthy control (HC, upper panels) and proband (Pt, lower panels).

#### **Supplementary Figure 11.**

Gating strategy for the identification of T-cells expressing phenotypic markers specific for Tfh (CXCR5 and PD-1) within the CD4, CD8 or DN T CD45RO<sup>+</sup> subsets in the lymph node of a healthy control (HC, upper panels) and proband (Pt, lower panels)

#### **Supplementary Figure 12.**

Gating strategy for the identification of NK cells (CD3 and CD56) and the expression of NK specific phenotypic markers (perforin, KIR, CD16 and NKG2D) in an healthy subject (HC), proband and her mother.

#### **Supplementary Figure 13.**

- a. Gating strategy for phenotypical and functional analysis of peripheral blood monocytes: monocytes were gated from cell aggregates, debris and other cell types based on their light scatter properties. Singlets were identified based on forward-scatter height and area and T, B and NK lymphocytes were excluded using a Dump channel for CD2, CD3, CD19, CD20 and CD56. HLA-DR expressing cells which did not acquire a viability dye were included for the phenotypic analysis of CD14 and CD16 expression
- b. Distribution of monocytes subsets as defined by CD14 and CD16 expression in 3 healthy control (HC, black symbols) and in the proband (Pt, red symbols). The median and 25-75<sup>th</sup> percentile IQR for the proportion of non-classical or patrolling monocytes



(CD14<sup>+</sup>CD16<sup>++</sup>, circles), intermediate (CD14<sup>++</sup>CD16<sup>++</sup>, square), classical monocytes (CD14<sup>++</sup>CD16<sup>-</sup>, diamond) is presented for 3 different HCs.

- c. Contour plot of fluorescence intensity vs side scattered light (SSC) of IL-6, TNF $\alpha$  and IL-1 $\beta$  intracellular staining in monocytes in resting conditions and upon LPS stimulation in fresh CD14<sup>+</sup> monocytes of healthy subject (HC, left panels) and proband (Pt, right panels). The blue plots in the left and right panels represent the distribution of fluorescence of cytokines intracellular staining in resting conditions in HC and proband's monocytes, respectively. The overlaid colored plots represents the distribution of fluorescence intensity of cytokines intracellular staining upon LPS stimulation in (HC, left panels) and proband (Pt, right panels).

#### **Supplementary Figure 14.**

Immunohistochemical staining of a lymph node in a healthy subject used a positive control:

- a. The brown staining highlights the CD4 expressing cells with single staining
- b. Dual staining for CD4 expressing cells (brown) and CD8 expressing cells (red) is presented.

Supplementary Table 1.

	Age (years)	4	8	15	16	18	21, 8 months	21, 11 months	22*	22, 4 months	23	Mother age 39
	<b>Normal values</b>											
<b>Weight (Kg)</b>		20	50	70	75	101	97.5	101.6	101.6	107.3	108.3	88
<b>Height (cm)</b>		102	130	169	169	169	169	169	169	169	169	171
<b>BMI</b>		19	29.6	24.5	26.3	35.4	34.1	35.6	35.6	37.6	37.9	30.1
<b>White blood cells</b>	4 -10.5 x10 <sup>9</sup> /μL	<b>15</b>	<b>12</b>	9.6	<b>11.7</b>	<b>13.8</b>	<b>12</b>	<b>12.4</b>	<b>32.7</b>	<b>13.13</b>	<b>12.15</b>	7.4
<b>Hemoglobin</b>	11.2-15.7 g/dL	11.3	12.8	12.8	13.4	13.4	14.6	13	13.6	14.1	14	13
<b>Platelets</b>	173-369 x10 <sup>9</sup> /μL	<b>402</b>	355	246	254	350	282	258	323	283	333	300
<b>Neutrophils (count, %)</b>	1600-6130/μL, 34-71%	<b>7650</b> , 51	5040, 42	4800, 50	<b>6318</b> , 54	<b>9232</b> , 67	<b>6360</b> , 53	4960, 40	<b>27795</b> , <b>85</b>	<b>7353</b> , 56	<b>6804</b> , 56	4800, 64
<b>Lymphocytes (count, %)</b>	1200-3740/μL, 1.2-52%	<b>6600</b> , 44	<b>5400</b> , 45	3552, 37	3243, 24	3569, 31	<b>4080</b> , 34	<b>6324</b> , 51	2060, 6	3584, 27	<b>3949</b> , 33	2040, 27
<b>Monocytes (count, %)</b>	240-860/μL, 4.7-12.5%	600, 4	<b>1080</b> , 9	768, 8	<b>1053</b> , 9	<b>911</b> , 7	840, 7	<b>868</b> , 7	<b>2616</b> , 8	<b>919</b> , 7	<b>863</b> , 7	460, 6
<b>Eosinophils (count, %)</b>	40-360/μL, 0.7-5.8%	15, 0.1	<b>444</b> , 4	<b>480</b> , 5	<b>646</b> , 6	<b>373</b> , 3	<b>720</b> , 6	<b>496</b> , 4	<b>0</b> , 0	<b>591</b> , 5	<b>462</b> , 4	70, 0.9
<b>CD3<sup>+</sup> T cells</b>	650-2800 /μL						2576	<b>3227</b>	1315	<b>3044</b>	2716	1528
<b>CD3<sup>+</sup>CD4<sup>+</sup> T cells</b>	370-1336 /μL						0	0	0	0	0	998
<b>CD3<sup>+</sup>CD8<sup>+</sup> T cells</b>	185-1024 /μL						<b>1933</b>	<b>2457</b>	1011	<b>2305</b>	<b>2086</b>	531
<b>B cells</b>	80-400 /μL								889	888	748	<b>403</b>
<b>NK cells</b>	126-841 /μL								<b>87</b>	215	472	170
<b>Immunoglobulin (Ig) G</b>	700-1600 mg/dL								1064	1075	1000	1073
<b>IgG1 subtype</b>	341-894 mg/dL										477	
<b>IgG2 subtype</b>	171-632 mg/dL										454	
<b>IgG3 subtype</b>	18.4-106 mg/dL										67.1	
<b>IgG4 subtype</b>	2.4-121 mg/dL								8.8		11.8	
<b>IgA</b>	70-400 mg/dL								343	269	276	248
<b>IgM</b>	40-230 mg/dL								115	79	89	114
<b>IgE</b>	0-90 IU/mL								<1	<1	1.3	1.9
<b>IgD</b>	<10 mg/dL										2	
<b>Protein C Reactive</b>	0-4.99 mg/dL								<b>15.9</b>	<b>7.2</b>		1.8

\*Acute presentation on September 2019 with multifocal pneumonia and hypoxic respiratory failure. Bold font indicates values outside the reference range.

Prior the episode of such acute presentation with hypoxic respiratory failure, the proband past medical history was significant for:

- Respiratory syncytial virus pneumonia requiring inpatient admission (1 month old).
- Rotavirus gastroenteritis at age 1.
- Diagnosis of attention deficit hyperactivity disorder at age 5-6 and currently managed with lisdexamfetamine
- Recurrent otitis media requiring myringotomy tubes (9 procedures) in childhood (6 episodes per year until age 4-5)
- Recurrent episodes of upper respiratory infection with productive cough (4-5 episodes per year): empiric course of antimicrobials, tonsillectomy and adenoidectomy.
- Multiple episodes of transient cervical lymphadenopathy during childhood.
- Onset of multiple skin warts at age 5-6: recalcitrant to topical treatment, cryotherapy and surgical excision. Spontaneously resolved around age 18-19.
- Varicella at age 6 despite receiving first dose of varicella vaccine at age 1.
- Recurrent episodes of back pain at age 15 with imaging significant for intervertebral herniations in the lower thoracic spine.

Supplementary Table 2.

Vaccine	Doses and Year	Titer
Hepatitis A	2 doses, 2008	Anti-HAV: Negative in 2020
Hepatitis B	3 doses, 1997-1998	Anti-HbS: Negative in 2020
Haemophilus Influenzae (Hib)	4 doses, 1997-1999	Anti-Haemophilus: <0.11 mg/L (minimal protective >0.15 mg/L) in 2020
Measles, Mumps, Rubella (MMR)	2 doses, 1999-2001	Mumps IgG: Negative in 2020; Measles and Rubella: Protective titers in 2020
Polio (IPV/OPV)	4 doses, 1997-2001	Poliovirus 1: 1:40 and Poliovirus 3: 1:20 (minimal protective titers >1:10) in 2020
Meningococcal (MPSV4)	1 dose, 2011	Serogroup A (0.9 µg/mL), C (<0.5µg/mL), Y (<0.5µg/mL), W (<0.5µg/mL) in 2020
Varicella zoster (Varivax)	1 dose, 1998	No repeat dose for extensive chickenpox in 2003, positive VZV IgG in 2020
Tetanus-Diphtheria-Pertussis (Tdap/Dtap)	6 doses, last 2011	Negative tetanus and diphtheria IgG 2019; positive 8 weeks after re-immunization in 2020
Pneumococcal (Prevnar, PCV7)	1 dose 2000	Protective titers in 16% (2/12) serotypes, 2019; 8 weeks after Pneumovax immunization in 2020: 69.5% (16/23) protective titers.

## Supplementary Methods:

### T-cells, monocytes, and B-cells phenotypic analyses

Peripheral blood mononuclear cells (PBMCs) were isolated by density centrifugation.

Monoclonal antibodies for the identification of T-cells and monocytes intracellular and extracellular antigens were: anti-CD3-BUV395 (BD), anti-CD8-APC (BD), anti-CD45-Krome Orange (BC), anti-CD3-PE (BC), anti-CD8-PB (BC), anti-CD2-V450 (eBioscience), anti-CD3-V450 (eBioscience), anti-CD19-V450 (eBioscience), anti-CD20-V450 (eBioscience), anti-CD56-V450 (BD), anti-HLA-DR-APC-cy7 (BD), anti-CD14-FITC (eBioscience), anti-CD16-PE-cy7 (BioLegend), anti-CCR5-APC-cy7 (BD), anti-CCR2-Percp-cy5.5 (BioLegend), anti-CX3CR1-APC (BD), anti-CD163-PE (R&D), anti-CD14-BV605 (BioLegend), anti-IL-6-APC (eBioscience), anti-PD-1-BV605 (BioLegend), anti-CCR7-FITC (R&D), anti-CXCR5-Percp-cy5.5 (BD), anti-CXCR3-PE (BD), anti-CD45RO-PE-cy7 (BD), anti-CD8-BV711 (BD), anti-CD3-V500 (BD), anti-CTLA4-APC (BD), anti-CD4-APC-cy7 (BD), anti-CD27-BV711 (BioLegend), anti-CD45RO-ECD (BC), anti-CD25-APC (BD), anti-Ki-67-FITC (BD), anti-FOXP3-PE (eBioscience), anti-CD28-PE-cy7 (eBioscience), anti-CD8-BUV395 (BD), anti-TCRV $\alpha$ 7.2-PerCP-Cy5.5 (BioLegend), anti-CD161-BV605 (BioLegend), anti-TCR $\alpha\beta$  BV421 (BioLegend), anti-CD27-FITC (BD), anti-TCR $\gamma\delta$  APC (BioLegend), anti-CD3-PE-Cy7 (BD), anti-CD40L(CD154)-PE (BD), anti-CD127-BV711 (BioLegend), anti-CD69 BV711 (BioLegend), anti-TNF $\alpha$ -FITC (BD), anti-IFN $\gamma$ -AF700 (BD), anti-IL-2 APC (BD), anti-Stat5 (pY694) Alexa Fluor 488 (BD), anti-CD3-PerCP-Cy5.5 (BD), anti-CD4-BV605 (BioLegend), IL17A-PE (eBioscience), anti-CD3-BUV661 (BD). Dead cells were identified and excluded using the LIVE/DEAD fixable Aqua, Near-IR, or Blue-Dead-Cell Stain kit (Invitrogen) while lymphocytes were identified according to their light-scattering properties.



Monoclonal antibodies for the identification of B-cells were CD20-allophycocyanin (APC)-H7 (clone 2H7, BD-Biosciences), CD19-PerCP-Cy5.5 (clone SJ25C1, Invitrogen), CD27-PE-Cy7 (clone O323, Invitrogen), CD21-FITC (clone Bu32, BioLegend), CD10-APC (clone HI10a, BD-Biosciences), CD38-BV-421 (clone HIT2, BD-Biosciences), and CD3-BV510 (clone OKT3, BioLegend). Lymph node mononuclear cells (LNMC) were isolated by mechanical disruption and filtered with a 70-um cell strainer. The following fluorochrome-conjugated monoclonal antibodies were used for B-cell staining of LNMC: CD19-PECy7 (clone SJ25C1, Invitrogen), CD27-BUV-395 (clone L128, BD-Horizon), CD38-BV421 (clone HIT2, BD-Biosciences), and CD3-BV650 (clone OKT3, BioLegend).

NK phenotype was evaluated by flow cytometry as based on expression of CD56, CD62L, CD94, CD117, CD16, and CD57. Flow-cytometry was performed on LSR-Fortessa (BD-Biosciences), with data analyses performed using FlowJo software (FlowJo LLC).

#### **NK phenotype and <sup>51</sup>Cr NK-cytotoxicity assay**

PBMCs were co-cultured with K562 target cells previously incubated with 100  $\mu$ Ci<sup>51</sup>Cr for 4 hours in a 96-well round-bottomed plate in the presence or absence of 1000 U/ml IL-2 (Roche). Following incubation, co-cultured cells were centrifuged, supernatant was transferred to a LUMA plate (Perkin Elmer) and dried overnight. Plates were read with a Top Count NXT and % specific lysis was calculated as follows:  $(\text{sample} - \text{average spontaneous release}) / (\text{average total release} - \text{average spontaneous release}) \times 100$ . Maximal release values were generated by lysis of target cells with 1% vol/vol IGEPAL (Sigma-Aldrich)[2].

NK phenotype was evaluated by flow cytometry to measure the surface expression of CD56-BV605 (Biolegend), CD62L-BV650 (Biolegend), CD94-APC (Biolegend), CD117-PE-Cy7 (Biolegend), CD16-PE-Texas-Red (BD Biosciences), NKG2D-PE-Cy7 (Biolegend), KIRs (CD158a, CD158b, CD158e cocktail, FITC, BD Biosciences), and CD57-BV510

(Biolegend), and intracellular expression of Perforin-BV711 (Biolegend). Data were acquired on a BD Fortessa or BD Celesta then exported to FlowJo (BD Biosciences) for analysis. NK cells were defined by FSC-SSC lymphocyte gating, then CD56<sup>+</sup>CD3<sup>-</sup>.

### **Cytokine production after in vitro-stimulation**

T-cells intracellular cytokine production was investigated by flow-cytometry upon stimulation with 2µg/mL CMV-pp65 peptide-pool, or 25µL/mL CMVGrade-2 lysate (Microbix Biosystems) and costimulatory antibodies (αCD28, αCD49d, BD-Biosciences). Briefly, cryopreserved PBMCs were thawed and resuspended in complete RPMI media (RPMI 1640 supplemented with 10% human AB serum, 50 µg/ml Gentamicin, and 1.7 mM L-glutamine), and rested for 2 hours at 37°C in the presence of 125U/mL benzonase (Sigma-Aldrich). Cells were then counted and plated as 10<sup>6</sup> cells/well in 96-well plates prior to stimulation with 2µg/mL CMV pp65 peptide pool, or 25 µL/mL CMV Grade 2 lysate (Microbix Biosystems) together with costimulatory antibodies (αCD28 and αCD49d; 1 µg/ml final concentration; Becton Dickinson). As a positive control, and for IL-17 induction, cells were treated with 25 ng/mL of phorbol 12- myristate 13-acetate (PMA; Sigma-Aldrich) plus 1 µg/mL of ionomycin (Sigma). For monocyte stimulation, cells were treated with 0.5µg/ml LPS (Sigma). 2 hours after stimulation, brefeldin-A (50µg/mL final concentration; Sigma-Aldrich) and monensin (0.7 µg/ml final concentration; BD-Biosciences) were added to block cytokine secretion. Cells were stimulated for 6 hours at 37°C in 5% CO<sub>2</sub>, and then stained following the flow cytometry assay described above.

### **Mixed Lymphocyte Reactions**

Cryopreserved PBMCs were thawed and rested for 2 hours at 37°C in presence of 125U/mL benzonase (Sigma-Aldrich). Monocytes from a healthy donor were sorted by using EasySep™ Human Monocyte Enrichment Kit without CD16 Depletion (Stemcell

Technologies) and used as stimulators. PBMCs from proband and a different healthy donor were labeled with 10 $\mu$ M CFSE and used as responders. Monocytes (stimulators) were plated as 5 x 10<sup>5</sup> cells/well in 24-well plate in presence or absence of Purified Mouse Anti-Human HLA-DR, DP, DQ (BD, Clone Tu39) and cultured at 37°C for 1 hour. Then CFSE-labeled responder cells were added to each well (5 x10<sup>5</sup> cells/well). MLR were cultured for 6 days when cell proliferation was measured by flow cytometry.

#### **Analysis of CD4 mRNA and DNA sequences.**

Purified PCR-product was sequenced with primers (**Supplementary Methods Table**) covering the full-length cDNA sequence (NM\_000616).

Genomic DNA of proband, and her mother, father and brother were extracted using AllPrep DNA/RNA Mini-Kit (QIAGEN). The exon 2 sequence, as well as its intronic flanking regions were analyzed by PCR amplification using 5'-

TCCAATTCCTCTGCTATTCTCCTG-3' and 5'TCTTTCCTGAGTGGCTGCTG-3' as forward and reverse primers, respectively. Purified PCR-products were sequenced using the same primers.

**Study Approval.** Participants were enrolled in the IRB-approved clinical protocol “Etiology and Pathogenesis and Natural History of Idiopathic CD4 Lymphopenia” (NCT00867269).

The B-cells phenotypic analysis was performed on PBMC and lymph nodes obtained from healthy and HIV-infected individuals enrolled in the clinical protocols: “Studies on Blood and Reproductive Fluids in HIV-Infected and Non-HIV-Infected Persons” (NCT00001281), “Leukapheresis procedures to obtain plasma and lymphocytes for research studies on primary and chronic HIV-infected-patients” (NCT00039689) and “Viral load in blood and lymph tissues of HIV-infected individuals” (NCT00001316). PBMC, sera and plasma from anonymous healthy persons were obtained through the NIH blood bank.

### Supplementary Methods Table 1:

<b>Primer</b>	<b>Sequence</b>
cDNA CD4 FP1	CTCTCTTCATTTAAGCACGACTCTGCAGAA
cDNA CD4 FP2	AGAGCTCCAAGTCCTCACACAGATAC
cDNA CD4 FP3	CCTGGTAGTAGCCCCTCAGT
cDNA CD4 FP4	GAGCCACTCAGCTCCAGAAA
cDNA CD4 FP5	GCCCCATTTGAGGCACGAGGC
cDNA CD4 RP1	CCCCTTGGACTCCTACATTGC
cDNA CD4 RP2	GGAGCTTAGGGTCCTGGGTA
cDNA CD4 RP3	CCTTGACTGGCTTGGCTGTGTG
cDNA CD4 RP4	GTAAGTTTATTGTATTTTTATTTCAG

### Supplementary material references

1. Zhang P, Bigio B, Rapaport F, et al. PopViz: a webserver for visualizing minor allele frequencies and damage prediction scores of human genetic variations. *Bioinformatics* **2018**; 34:4307-9.
2. Gunesch JT, Dixon AL, Ebrahim TA, et al. CD56 regulates human NK cell cytotoxicity through Pyk2. *Elife* **2020**; 9.